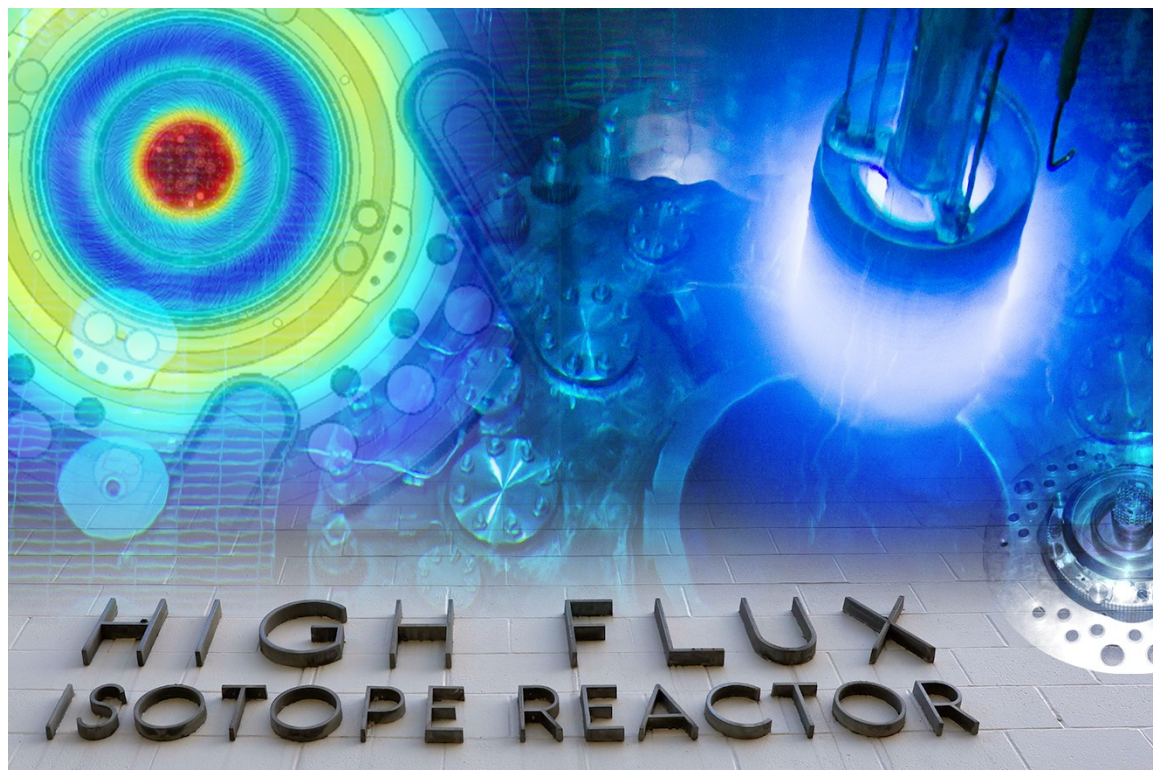


# Volume 4: Detection Systems and Ultra-Cold Neutrons

## HFIR Futures – Enhanced Capabilities Series



Gale Hauck  
Mitch Allmond  
Leah Broussard  
David Glasgow  
Callie Goetz  
Jason Gardner  
Zain Karriem  
Padhraic Mulligan

**January 2023**

## DOCUMENT AVAILABILITY

Reports produced after January 1, 1996, are generally available free via OSTI.GOV.

**Website** [www.osti.gov](http://www.osti.gov)

Reports produced before January 1, 1996, may be purchased by members of the public from the following source:

National Technical Information Service  
5285 Port Royal Road  
Springfield, VA 22161  
**Telephone** 703-605-6000 (1-800-553-6847)  
**TDD** 703-487-4639  
**Fax** 703-605-6900  
**E-mail** [info@ntis.gov](mailto:info@ntis.gov)  
**Website** <http://classic.ntis.gov/>

Reports are available to DOE employees, DOE contractors, Energy Technology Data Exchange representatives, and International Nuclear Information System representatives from the following source:

Office of Scientific and Technical Information  
PO Box 62  
Oak Ridge, TN 37831  
**Telephone** 865-576-8401  
**Fax** 865-576-5728  
**E-mail** [reports@osti.gov](mailto:reports@osti.gov)  
**Website** <https://www.osti.gov/>

This report was prepared as an account of work sponsored by an agency of the United States Government. Neither the United States Government nor any agency thereof, nor any of their employees, makes any warranty, express or implied, or assumes any legal liability or responsibility for the accuracy, completeness, or usefulness of any information, apparatus, product, or process disclosed, or represents that its use would not infringe privately owned rights. Reference herein to any specific commercial product, process, or service by trade name, trademark, manufacturer, or otherwise, does not necessarily constitute or imply its endorsement, recommendation, or favoring by the United States Government or any agency thereof. The views and opinions of authors expressed herein do not necessarily state or reflect those of the United States Government or any agency thereof.

HFIR SENSE LDRD

**VOLUME 4: DETECTION SYSTEMS AND ULTRA-COLD NEUTRONS**

**HFIR FUTURES – ENHANCED CAPABILITIES SERIES**

Gale Hauck  
Mitch Allmond  
Leah Broussard  
David Glasgow  
Callie Goetz  
Jason Gardner  
Zain Karriem  
Padhraic Mulligan

January 2023

Prepared by  
OAK RIDGE NATIONAL LABORATORY  
Oak Ridge, TN 37831-6283  
managed by  
UT-BATTELLE LLC  
for the  
US DEPARTMENT OF ENERGY  
under contract DE-AC05-00OR22725

## CONTENTS

LIST OF FIGURES .....	iv
LIST OF TABLES .....	iv
ABBREVIATIONS .....	v
ACKNOWLEDGMENTS .....	vi
ABSTRACT .....	1
1. BACKGROUND OF THE HIGH FLUX ISOTOPE REACTOR ENHANCED CAPABILITIES SERIES REPORTS .....	1
2. WORKING GROUP OBJECTIVES AND GOALS .....	2
2.1 DESCRIPTION OF WORKING GROUP .....	2
3. CONCEPTUAL DESIGN DEVELOPMENT .....	2
3.1 FAST ACCESS DETECTION SYSTEMS .....	3
3.1.1 Impact .....	3
3.1.2 Comparison to Other Facilities .....	4
3.1.3 Design Requirements .....	4
3.1.4 Limitations/Challenges .....	5
3.1.5 Calculations .....	5
3.1.6 Cost Forecasting and Estimates .....	7
3.1.7 Schedule Planning and Estimates .....	7
3.2 NON-SCATTERING BEAMLINE INSTRUMENTS .....	8
3.2.1 Neutron Depth Profiling .....	8
3.2.2 PGAA and Prompt Gamma Imaging .....	11
3.3 SHIELDED DETECTION INSTRUMENTS .....	13
3.3.1 The HFIR Decay Station (HDS) .....	13
3.3.2 Precision Frontier of Science and Applications Enabled by the HDS .....	15
3.3.3 Preliminary Design and Configuration Concepts of the HDS .....	16
3.3.4 ORNL Expertise and Leadership on HDS-Style Arrays .....	17
3.3.5 Comparison of HDS with Similar Arrays and Facilities .....	17
3.3.6 HDS Footprint, Requirements, and Possible Locations .....	18
3.3.7 HDS Operations and Access .....	18
3.3.8 HDS Cost and Schedule Profile .....	19
3.4 ULTRACOLD NEUTRON SOURCE .....	19
3.4.1 Overview of Current Ultracold Neutron Sources .....	20
3.4.2 Neutron Fluxes on HFIR Beam Tubes .....	24
3.4.3 Design Requirements .....	25
3.4.4 Limitations/Challenges .....	25
3.4.5 Impacts to HFIR .....	25
3.4.6 Scoping Analyses .....	26
4. CONCLUSION .....	32
5. REFERENCES .....	32

## LIST OF FIGURES

Figure 1. Candidate designs for PT-1 in-pool detector array.....	6
Figure 2. Candidate design for PT-2 ex-pool detector array located on the fast-transfer pneumatic tube system.....	6
Figure 3. Candidate arrangement of the ex-pool PT-2 detector array.....	7
Figure 4. Illustration of charged particle reaction used in neutron depth profiling. ....	8
Figure 5. Conceptual design of NDP instrument for HB-3 beam station. ....	10
Figure 6. Conceptual design of a PGAA facility on a HFIR beamline.....	12
Figure 7. Two histograms showing a measurement with the CLARION detector of a silver foil that was irradiated within HFIR [Gross et al. 2000]:.....	14
Figure 8. HDS within a wider context of ORNL capabilities. ....	16
Figure 9. Preconceptual HDS designs and configurations for enabling complete spectroscopy of gamma, neutron, and charged-particle radiation with ultra-sensitivity to weak decay signatures. ....	16
Figure 10. Recent HDS-style arrays (but previous generation) built and led by ORNL: .....	17
Figure 11. Gamma-ray detection efficiencies of HPGe arrays in North America: DEGA-HDS is the top red line with the highest efficiency. ....	18
Figure 12. WWR-M thermal column UCN source design (large collection of low flux in thermal column) [Serebrov et al. 2017]. ....	23
Figure 13. PIK beam tube UCN source design (low collection of flux in small GEK-3 and GEK-4 tubes) [Serebrov et al. 2016]. ....	23
Figure 14. HFIR thermal flux map.....	24
Figure 15. MCNP model showing HFIR beam lines and location types where neutron currents were calculated.....	27
Figure 16. HFIR HB beam tube currents. ....	28
Figure 17. HFIR MCNP model with large HB-2 tube. ....	29
Figure 18. HFIR MCNP model with large HB-2 tube. ....	29
Figure 19. EF-1 facility. ....	31
Figure 20. EF-1 Facility with MCNP model overlayed onto HFIR drawing. ....	31
Figure 21. EF-1 neutron current results. ....	32

## LIST OF TABLES

Table 1. Summary of the HFIR Futures – Enhanced Capabilities Series .....	2
Table 2. Comparison of operating and planned UCN sources.....	22
Table 3. HFIR HB beam tube currents and fluxes .....	27
Table 4. Neutron currents and fluxes for 60 cm diameter HB-2 concept. ....	30

## ABBREVIATIONS

BESAC	Basic Energy Sciences Advisory Committee
CZT	cadmium zinc telluride
DOE	US Department of Energy
FDSi	FRIB Decay Station initiator
FIPPS	Fission Product Prompt Gamma-Ray Spectrometer
FRIB	Facility for Rare Isotope Beams
FSU	Florida State University
HDS	HFIR Decay Station
HEU	highly enriched uranium
HFIR	High Flux Isotope Reactor
HPGe	high purity germanium
ILL	Institut Laue-Langevin
LaBr <sub>3</sub>	lanthanum bromide
LDRD	Laboratory Directed Research and Development
LEU	low-enriched uranium
MCNP	Monte Carlo N-Particle
MURR	Missouri University Research Reactor
NAA	Neutron Activation Analysis [lab]
NDP	neutron depth profiling
nEDM	neutron electric dipole moment
NIST	National Institute of Standards and Technology
OLIF	On-Line Isotope Facility
ORNL	Oak Ridge National Laboratory
PGAA	prompt gamma neutron activation analysis
PGI	prompt gamma imaging
PNPI	Petersburg Nuclear Physics Institute
PT	pneumatic tube
REDC	Radiochemical Engineering Development Center
RIB	radioactive ion beam
RPV	reactor pressure vessel
SC	Office of Science
SENSe	Sustaining and Enhancing Nuclear Science
TRL	technology readiness level
UCN	ultracold neutron

## **ACKNOWLEDGMENTS**

Research sponsored by the Laboratory Directed Research and Development Program of Oak Ridge National Laboratory, managed by UT-Battelle, LLC, for the US Department of Energy under contract DE-AC05-00OR22725. The authors would like to acknowledge Chris Bryan and Randy Belles of Oak Ridge National Laboratory for their comprehensive technical reviews of this paper.

## ABSTRACT

As part of the Sustaining and Enhancing Nuclear Science (SENSe) initiative at Oak Ridge National Laboratory (ORNL), the prospect of adding new detection systems to support High Flux Isotope Reactor (HFIR) operations and to advance scientific research has prompted many ideas and discussions regarding potential features, configurations, locations, and applications. A working group of ORNL staff members was organized to further develop the concepts and recommending one or more configurations to best support future HFIR operations and scientific capacities and to provide order-of-magnitude cost estimates and timing. The areas of investigation included fast access detection systems, non-scattering beamline instruments, shielded detection instruments, and an ultracold neutron source. In each case, the focus was to develop world leading capabilities that would be unmatched by any other facility.

### 1. BACKGROUND OF THE HIGH FLUX ISOTOPE REACTOR ENHANCED CAPABILITIES SERIES REPORTS

In 2019, the US Department of Energy (DOE) Office of Science (SC) chartered the Basic Energy Sciences Advisory Committee (BESAC) to assess scientific justification for a domestic high-performance reactor-based research facility. This committee delivered a report with specific recommendations focused on (1) continuing operations beyond the year 2100, (2) enabling future additional scientific capabilities, and (3) converting the reactor to low-enriched uranium (LEU) [BESAC 2020]. The review determined that HFIR will have a critical role in the future of US neutron science research and recommended the immediate pursuit of scientific enabling enhancements, including replacement of the reactor pressure vessel (RPV), conversion to LEU fuel, enhanced capabilities for in-core irradiations and neutron scattering research, modifications to the fuel assembly, and restoration of the flux intensity of the original 100 MW highly enriched uranium (HEU) operations.

In response to the BESAC report, Oak Ridge National Laboratory (ORNL) funded an initiative to provide a critical assessment of the hardware, systems, and infrastructure required to sustain and enhance HFIR capabilities. The HFIR Sustaining and Enhancing Neutron Science (SENSe) initiative consists of three Laboratory Directed Research and Development (LDRD) projects assessing (1) infrastructure enabling operation past 2100, (2) non-neutron-scattering scientific capability enhancements and planning, and (3) neutron scattering scientific capability enhancements and planning. The report by Bryan and Chandler [Bryan 2022] provides more information regarding HFIR, BESAC report recommendations, the HFIR-SENSe initiative, and the goals of the three LDRDs.

The effort to brainstorm nonscattering scientific enhancements at HFIR was a “blue-sky” engagement with researchers across ORNL and has yielded incremental improvement ideas, as well as concepts for new transformational capabilities. To initiate the effort, 35 concepts were grouped into 13 separate working groups. The goal of each group was to further develop the concepts, build a scientific justification, identify potential sponsors, and estimate costs and schedules for each concept. This effort culminated in this multivolume series of documents that summarizes these efforts and ideas.



Table 1 itemizes these volumes.

**Table 1. Summary of the HFIR Futures – Enhanced Capabilities Series**

<b>Volume</b>	<b>Report number</b>	<b>Volume title</b>
1	ORNL/TM-2022/2691/V1	Volume 1: Introduction to the HFIR Futures - Enhanced Capabilities Series
2	ORNL/TM-2022/2691/V2	Volume 2: Hot Cells Connected to the Reactor Pool
3	ORNL/TM-2022/2691/V3	Volume 3: Online Insertion and Removal Facilities
4	ORNL/TM-2022/2691/V4	Volume 4: Detection Systems and Ultra-Cold Neutrons
5	ORNL/TM-2022/2691/V5	Volume 5: Flexible Flux Trap Configurations
6	ORNL/TM-2022/2691/V6	Volume 6: Experiment Facility Spectrum Tailoring
7	ORNL/TM-2022/2691/V7	Volume 7: Cryogenic Facility
8	ORNL/TM-2022/2691/V8	Volume 8: Epithermal and Fast Neutron Radiography Facility
9	ORNL/TM-2022/2691/V9	Volume 9: Critical Facility with Add-On Ion Beam
10	ORNL/TM-2022/2691/V10	Volume 10: Flow Test Facilities
11	ORNL/TM-2022/2691/V11	Volume 11: Modeling & Simulation
12	ORNL/TM-2022/2691/V12	Volume 12: Flow Loop Facilities
13	ORNL/TM-2022/2691/V13	Volume 13: Neutrino Facilities

## **2. WORKING GROUP OBJECTIVES AND GOALS**

### **2.1 DESCRIPTION OF WORKING GROUP**

The HFIR SENSE initiative provided a unique, transformational opportunity to explore new scientific capabilities at ORNL. Several new infrastructure and instrumentation techniques were proposed and categorized as HFIR detection systems. These included:

- a fast access detection system for performing rapid neutron and gamma measurements on pneumatic tube experiments exiting the reactor,
- a neutron depth profiling (NDP) instrument,
- a prompt gamma neutron activation analysis (PGAA) instrument,
- a high resolution, high detection efficiency decay station, and
- an Ultracold Neutron source.

To develop these concepts, staff from multiple ORNL divisions met virtually on a biweekly basis to discuss and present brainstorming efforts. This report describes these detection system concepts and presents the associated high-level designs, added benefits, and procurement estimates for further development.

## **3. CONCEPTUAL DESIGN DEVELOPMENT**

The detection systems proposed as part of the HFIR SENSE initiative were grouped into three general categories: fast access detection systems, non-scattering beamline instruments, and shielded detection

instruments. In addition, a proposed ultra-cold neutron source is discussed. Details for each of these scientific enhancements are provided in the following sections.

### **3.1 FAST ACCESS DETECTION SYSTEMS**

To fully support the need for rapid access to detector arrays following neutron irradiation, two distinct detector arrays are proposed. The first array is considered a medium-activity array of combined neutron/gamma-ray detectors for use after irradiation of the experiment in the pneumatic tube. This detector array will have a sensitivity between that of the highly sensitive decay station and that of the collimated high activity station within the HFIR pool. Consequently, this detector array design requires adequate shielding; flexibility to be reconfigured for different sample types, irradiation conditions, and experiments; and availability to the current pneumatic tube (PT)-2 fast transfer rabbit tube. Originally evaluated as an in-pool detector array, this detection station is better served as a modular ex-pool decay station on the PT-2 sample transfer system in the Experiment Room adjacent to the reactor pool, as shown in Figure 3.

The second proposed detector station is a high-activity array designed to remain in-pool. It is a simpler gamma-ray and dose rate measurement station intended to be stationed on PT-1, which is unique among high-flux irradiation stations because it has the capability to stop the rabbit at a measurement location for a predetermined period before it is returning it to the loading station in the laboratory. This location is just above the grating in the reactor pool, close to the current waiting station where capsules may be halted inside the pool, allowing time to decay, ahead of moving into the Neutron Activation Analysis (NAA) lab for processing.

Because the components near the grating level in the pool are inaccessible during reactor operation, only the most robust systems for gamma-ray and neutron measurement are considered for the in-pool station. For example, noncryogenic detectors are preferred and would be arranged in coincidence/anticoincidence geometry to facilitate counting of high-count-rate samples. The detector signals will be processed digitally using loss-free counting techniques to address changing detector deadtime during measurement. In this way, neutron counting, gamma-ray spectrometry, and dose rate analysis of irradiated materials are facilitated entirely without bringing the sample back to the laboratory.

Expected transfer times for samples from the irradiation site to the detector could be as low as 1 second, so access to delayed neutron groups and short-lived fission and activation products is facilitated by counting in the pool with complete safety. Virtually any quantity of radioactive material could be addressed in this counter without the risk of manual handling in the laboratory. Dose rate measurements would ensure that sufficient decay is allowed before the sample is returned to the laboratory. For samples with very high radioactivity, collimated and/or layered detectors would be employed to reduce count rates to acceptable levels. Finally, the highest quality spectra will likely be obtained by using shielding on all sides to reduce down-scattered radiation from the water. The detector signals will exit the pool through one of the cable penetrations into the Experiment Room NAA Lab for digital processing.

#### **3.1.1 Impact**

This combination of the highest thermal neutron flux in the world and in-line gamma and neutron detection capability has no peer in such a system. The magnitude of the thermal flux makes the radioactivity generation rate in the PT-1 superior at approximately  $\frac{1}{2}$  of the HFIR peak flux. A detector capable of high-rate counting in a large background is needed to address short-lived intermediates in a variety of isotope production, forensic, and materials characterization applications. Significant contributions to fundamental science are anticipated in diverse areas of research, including nuclear data and advancing isotope production schemes through measurement of radioactive intermediates. The high

flux and inline counter will be especially useful in the analysis of trace and matrix compositions in extremely small and refractory solid samples. These samples will include lunar and meteoritic materials, ultra-high purity silicon, and  $^{238}\text{Np}$ , an intermediate in the production of  $^{238}\text{Pu}$  [Romano et al. 2022]. The short travel time to the counter has significant advantages for the characterization of short-lived fission products from exotic actinides and for the determination of short-lived activation products with the highest sensitivity available to the neutron activation analysis technique.

### 3.1.2 Comparison to Other Facilities

There is no analogue for this proposed detector array, a modular detector array capable of simultaneous neutron and gamma measurements that can be rapidly accessed by a high-flux neutron irradiation position. In the United States, the National Institute of Standards and Technology (NIST) and Missouri University Research Reactor (MURR) are two high-flux reactors with robust NAA programs, but they do not have this capability. There are examples of such fast transfer systems connected to neutron generators, but their fluence rates are lower at approximately  $10^8 \text{ n/cm}^2/\text{s}$ . However, they have demonstrated transfer times as low as 400 ms. In Europe, the JSI reactor in Slovenia has a 1-second transfer time but operates at only 250 kW, so the neutron flux is only in the  $10^{12} \text{ n/cm}^2/\text{s}$  range [Johns and Nino 2019]. The HFIR fast-transfer system could deliver a sample to the ex-pool detector array in approximately 300 ms and would likely be the fastest transfer system in the world.

The existing PT facilities at HFIR contain a unique design feature: both PT-1 and PT-2 have decay positions near the pool grating that can accept high amounts of short-lived radionuclides for decay before returning the sample back to the laboratory. This feature will be used to stop a rabbit at the PT-1 in-pool decay station for measurement. There is sufficient space for a detector array near the west pool wall to facilitate this upgrade, and the PT system logic fully supports it.

### 3.1.3 Design Requirements

For this upgrade, it is assumed that PT-1 will require minimal or no changes to preserve its safety functions. Therefore, the addition of a measurement station on PT-1 should fit into the current design to the extent possible. Additionally, it is assumed that the NAA laboratory reconfiguration plan to move closer to the west pool wall in the Experiment Room will have been accomplished. This will facilitate implementing the measurement station on the fast-transfer system on PT-2. This discussion adheres to the constraints of these two assumptions.

Two measurement stations are being considered. The station on PT-1 will be submersible and is intended to be serviceable during reactor outages. Therefore, the detectors and associated umbilical must be robust and capable of achieving low failure rate. This array should consist of high-rate detectors of modest size and may include cadmium zinc telluride (CZT) semiconductors, lanthanum bromide ( $\text{LaBr}_3$ ) scintillators, or other solid-state detectors that can function effectively at the pool temperature rather than being cryogenically assisted [Smodis and Snoj 2011]. The detectors could be configured as rings of layered modules with inner and outer detector segments. For lower rate measurements, the entire detector volume could be used for increased detection efficiency. In the case of high-rate measurements, the data from the inner module could be discarded, with only data from the outer modules being collected. This approach would allow the inner modules to effectively shield the outer modules, enabling both high- and low-rate counting without changing the in-pool detector geometry. Detector segmentation will facilitate coincidence/anticoincidence measurements and construction of decay schemes [Goetz 2017].

$^3\text{He}$  neutron detectors provide superior rejection of gamma-ray pulses and capability to perform coincidence / anticoincidence measurements to reduce the background radiation. In addition, down-scattered radiation from the reactor must be shielded to keep the background count rate manageable. A

steel encapsulated Pb shield can be placed on the pool grating; if it cannot be supported because of weight capacity, then the detection array could be positioned higher up the pool wall to be further from the reactor and to lessen the background. An ion chamber detector will also be included to observe dose rate changes during counting. The detector will also be used to ensure that samples have arrived at the detector array and that they have decayed to safe levels before they are returned to the lab. A dose meter solves several challenges of the current system and is a welcome addition.

The second measurement station, located on a potential large-bore fast rabbit PT-2 system (ORNL/TM-2022/2691/V3, Online Insertion and Removal Facilities), is accessed within ~300 ms of the end of irradiation. This station will combine high-resolution gamma spectrometry with neutron multiplicity and energy discrimination in a novel modular multidetector sensor array. The new measurement array will contain  $^3\text{He}$  detectors arranged in concentric rings to reject gamma-ray pulses, to facilitate multiplicity measurements, and to support delayed neutron counting. Furthermore, a wide variety of detection systems may be employed in the modular design to accommodate all current missions while reserving the capacity to address detector development, nuclear data, and analytical needs into the future. The key is in the modular design. The ability to customize shielding and geometry for counting provides the potential for detector development and exploitation of short-lived intermediates for nuclear data improvement. This array can accept a variety of collimators to address portions of the irradiated rabbit to determine neutron fluence gradients and to allow for comparator analysis without opening the irradiation container.

#### **3.1.4 Limitations/Challenges**

Data handling presents a potential challenge with these detection systems. To automate irradiation and materials analysis, fast, accurate data reduction strategies must be developed to handle the throughput [IAEA 2018]. Timing issues may also be significant in some cases. For example, precisely timing the start and end of the irradiation down to the low millisecond scale is not a simple feat. This challenge can be partially mitigated by using reference monitors that yield gamma or neutron radiation without interfering with the measurements. In this way, a witness sample can be used to correct or normalize time differences. However, this method is not possible in all situations. Automation of the irradiation and analysis of materials is highly desirable but is also quite difficult. In fact, full automation of NAA facilities around the world is very rare. The best example is at Delft in the Netherlands, where they have automated most portions of the NAA method, but not within the short time regime in which the HFIR upgrade detector array will operate.

#### **3.1.5 Calculations**

Only a few general arrangements that can be accommodated for the in-pool detection stations. As shown in Figure 1 left, the PT-1 flight tube is surrounded by graded shielding, collimator, and moderator (or shield) to accomplish simultaneous neutron, gamma-ray, and dose rate analysis. A layered array is shown on the right, where the inner modules may be used to collect data in lower rate samples or as shielding for the outer modules for high-rate collections. In both possible configurations, this array would need significant shielding on its exterior to reduce ambient radiation, as well as on its interior to accommodate high-radioactivity samples. Therefore, CZT and  $\text{LaBr}_3$  were the chosen detector types because of their operation at room temperature, tolerance of high count rates, and small size.

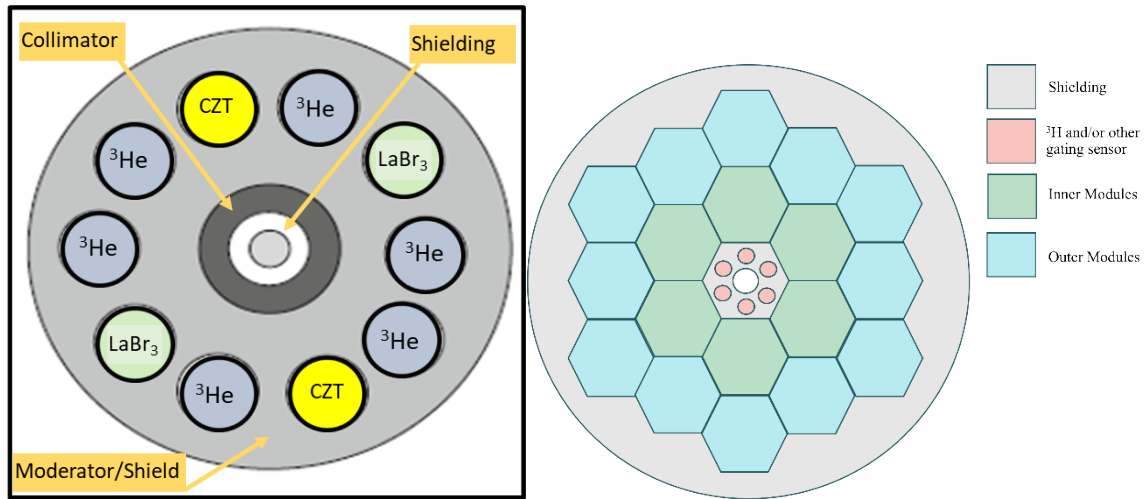


**Figure 1. Candidate designs for PT-1 in-pool detector array.** The choice of detectors and physical arrangement will be determined through modeling and according to the dimensions and geometries of the shields and collimators. A desirable feature would be the capability to select different distances for the detectors from the sample to accommodate count rates, which are expected to vary widely.

The PT-2 detector array design is expected to be modular to accommodate detector development and analytical performance. Figure 2 depicts one vision of this array with medium- and high-resolution detectors that can be cryogenically cooled. The shielding and detector frame/support would be stacked to accommodate additional detector designs. The goal is to achieve 40% neutron detection efficiency, as well as simultaneous gamma singles and coincidence spectra, as a minimum.

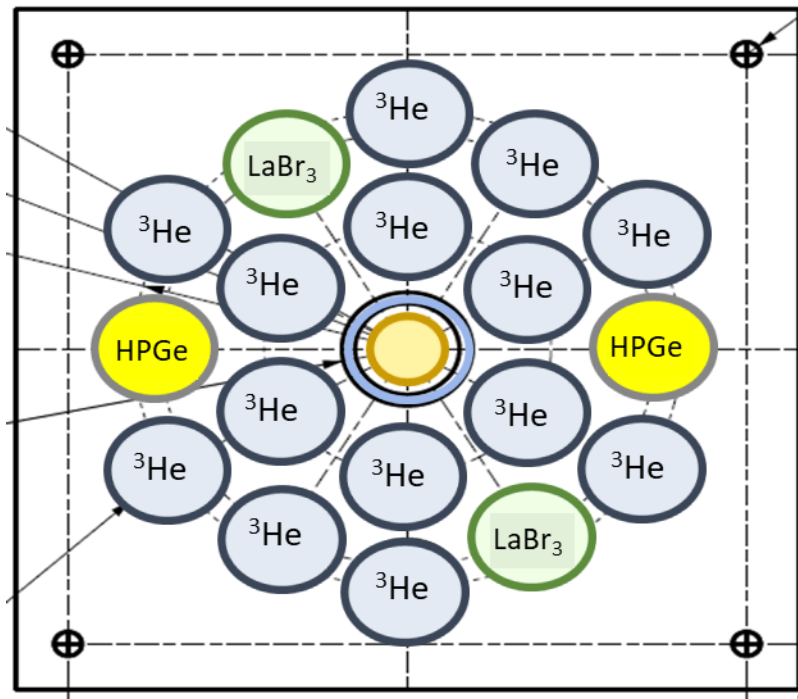


**Figure 2. Candidate design for PT-2 ex-pool detector array located on the fast-transfer pneumatic tube system.** Signals processing would be closely tied to the logic operator for the pneumatic transfer system to accomplish rapid acquisition of data that are timed well to address cyclic, static, and more exotic sample handling routines.

The PT-2 detector array will require heavy shielding because of its proximity to the pool wall and neutron scattering facilities in the beam room below. Its position on the heavy biological shield monolith effectively eliminates floor loading concerns. Background data taken recently as part of the neutrino detection experiments in the experiment room will be used as input to an analysis to determine the detector's location. Ideally, the detector should be as close to the reactor as possible to ensure that the rabbit can be transferred from the reactor to the counter in 0.5 seconds or less to analyze short half-life intermediates and delayed neutron groups.

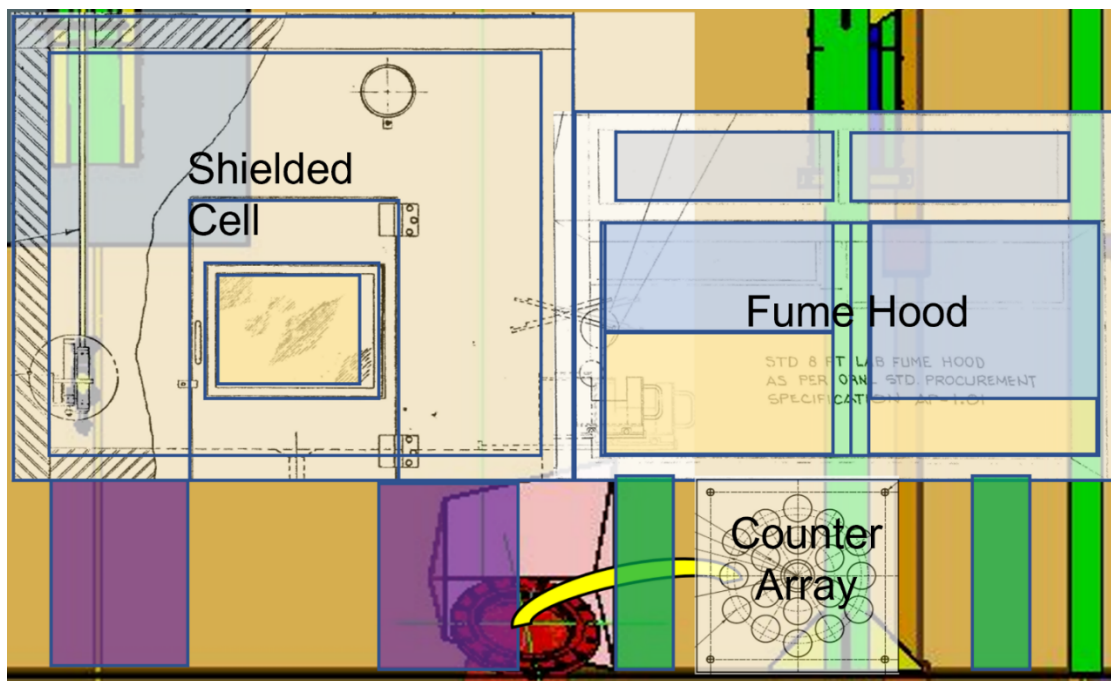


**Figure 3. Candidate arrangement of the ex-pool PT-2 detector array.** The existing hood and shielded cell, which will be relocated to the monolith, are also depicted.

### 3.1.6 Cost Forecasting and Estimates

The cost of the PT-1 detector array is expected in the range of \$1–1.25M, most of which will be for modeling and design and not the detectors themselves. Installation is also expected to be more for this array because of factors in the reactor pool work environment.

The PT-2 detector array could cost \$2–3M because the detectors will be more expensive, but the installation will be less complex. Modeling and design and implementation of modular features, as well as implementation of automation and data handling specifications, will comprise a significant part of the costs.

### 3.1.7 Schedule Planning and Estimates

During installation of the PT-1 detector array, HFIR must be in outage and the reactor pool drained to allow access to the areas just above grating level. Also, the loading limits for the grating must be evaluated against the weight of the gamma-ray shielding to ensure that they are sufficient.

## 3.2 NON-SCATTERING BEAMLINE INSTRUMENTS

As part of the proposed HFIR scientific enhancements initiative, a new thermal neutron guide hall will be commissioned to expand neutron scattering instrument capabilities at ORNL. These proposed instruments will be detailed in a future neutron scattering scientific capability enhancements report. The following section describes several new non-scattering beamline instruments for a new thermal guide hall which would introduce new capabilities to ORNL and the DOE Office of Science instrument portfolio. The proposed additional capability will include neutron depth profiling and prompt gamma neutron activation analysis and imaging.

### 3.2.1 Neutron Depth Profiling

Nondestructive depth-resolved measurement of impurities in thin films is an increasingly important analytical technique in materials, solar energy, and Li-ion energy storage research. NDP is a well-established [Ziegler et al. 1972] [Downing and Lamaze 1995] technique for these measurements. NDP uses thermal or cold neutrons to induce charged particle reactions in a material of interest. Following neutron capture (Figure 4), these particles and recoil nuclei are generated with known energy based on the Q-value of the reaction. The particles travel out of the sample material, losing energy along their trajectory. Detecting the residual energy of these particles in vacuum provides a charged particle energy spectrum of the sample which can be unfolded using the material's stopping power to reveal a depth-resolved concentration profile in the sample. Although this approach is limited to analysis of specific isotopes which undergo charged particle reactions ( $^3\text{He}$ ,  $^6\text{Li}$ ,  $^{10}\text{B}$ , and several others) its use has increased using the instruments recently constructed at research reactors in China [Chanjuan et al. 2019], India [Mandal et al. 2020], South Korea [Park et al. 2014], Germany [Vezhlev et al. 2020] [Werner et al. 2018], and the United States [Mulligan et al. 2012].

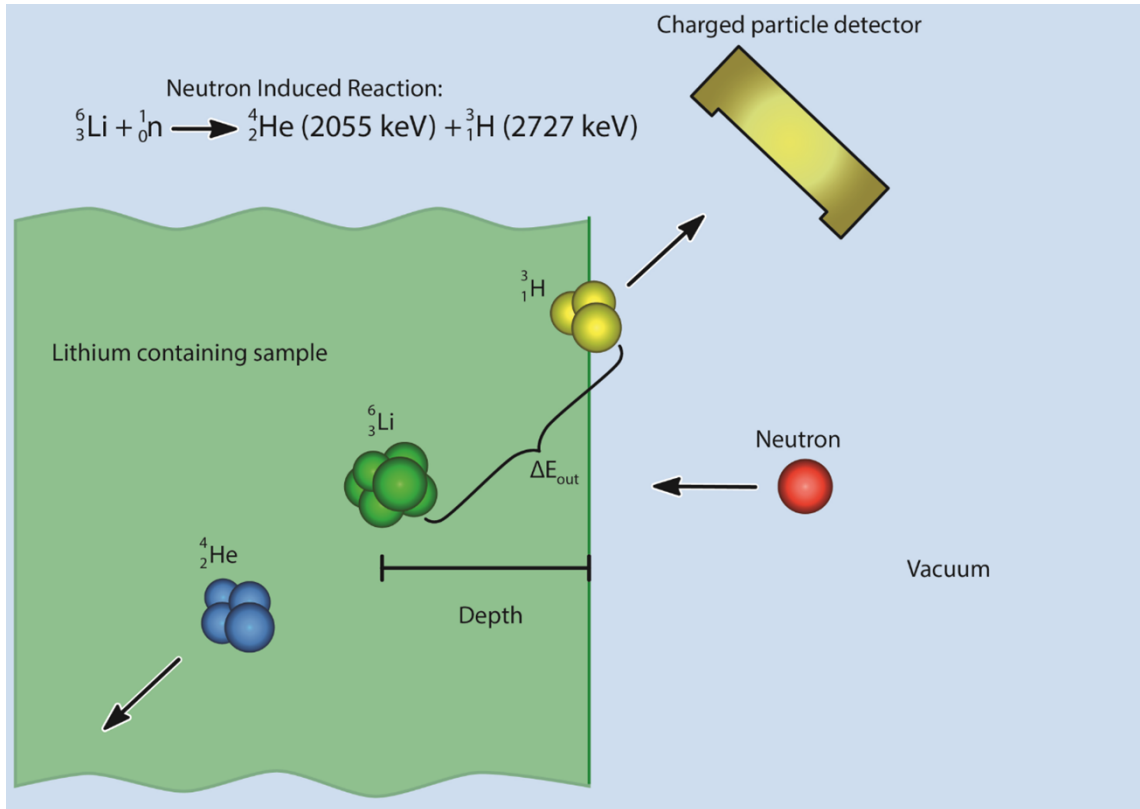


Figure 4. Illustration of charged particle reaction used in neutron depth profiling.



### 3.2.1.1 NDP Instrument Concept

The proposed NDP instrument requires the use of a new cold or thermal neutron beam line. A thermal or cold neutron spectrum is required to prevent momentum transfer to the target nucleus, which would distort measurement of the sample's true concentration profile. Any of the HFIR beamlines provides sufficient thermal neutron flux to make the proposed instrument competitive with other NDP user facilities, but a cold neutron spectrum would increase the reaction rate because of the  $1/v$  dependence of the capture cross section, significantly improving the lower limits of detection.

The conceptual instrument consists of a large ( $\sim 1 \text{ m}^3$ ) ultra-high vacuum chamber centered in the beamline with thin aluminum windows to allow passage of the neutron beam through the chamber with minimal scattering or attenuation. A  $^6\text{Li}$ -enriched glass aperture would be used to reduce the beam area to  $1 \text{ cm}^2$  before impinging upon a sample mounted in the center of the vacuum chamber. An array of ten high-resolution charged particle detectors located at the periphery of the vacuum chamber would face the mounted sample to detect neutron-induced charged particle reactions. Multiple detectors would increase the instrument's efficiency by (1) requiring less time to acquire statistically significant measurements and (2) allowing more samples to be analyzed while HFIR is operating. During instrument operation, the chamber would be evacuated to ultra-high vacuum pressure ( $10^{-6} \text{ Pa}$ ), thus requiring a turbomolecular vacuum pump. Excluding the required infrastructure for any beamline instrument (beam shutter, beam stop, shielding, etc.) the standalone NDP instrument would require  $1\text{--}2 \text{ m}^2$  of floorspace and would easily fit within a  $5 \times 5 \text{ m}$  experiment station. Additional space would also be needed for vacuum pumps, pressure gauges, and associated detector electronics; but these could be located at some distance from the instrument. Because the sample would be small and the reactions of interest would be charged particle reactions, shielding requirements would be minimal. A schematic of a representative NDP instrument is shown in Figure 5.

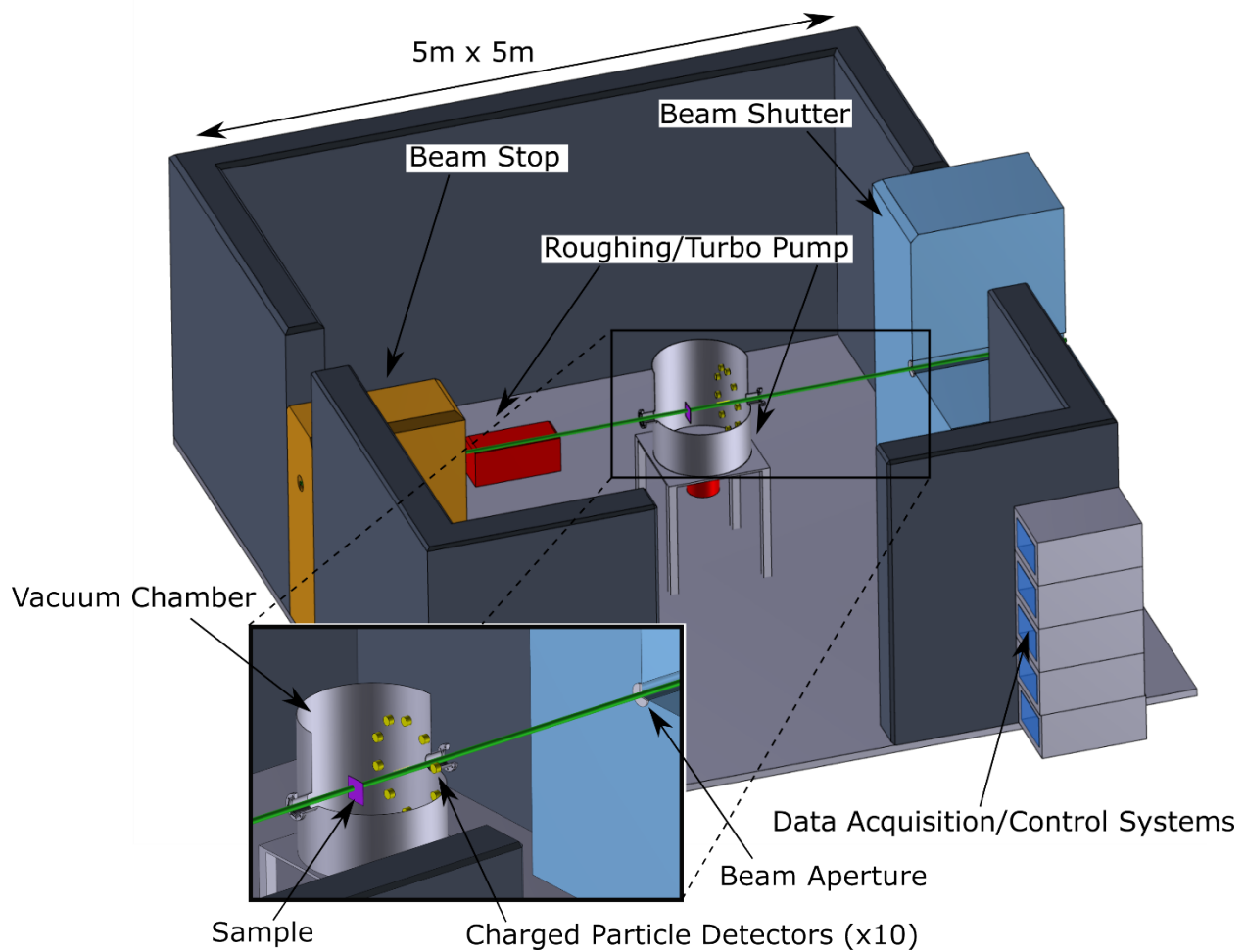


**Figure 5. Conceptual design of NDP instrument for HB-3 beam station.**

### 3.2.1.2 Benefits of an NDP Facility

An NDP instrument at HFIR would provide new capabilities in a wide range of research areas. NDP brings new capabilities to nondestructively quantify the concentration of certain light isotopes on the surfaces of new materials or devices. NDP can be used to profile static materials such as doped semiconductors [Downing and Lamaze 1995], biological samples, novel thin film materials [Wang et al. 2017], and helium accumulation in fusion materials. Recently, NDP has experienced a resurgence as a nondestructive analytical technique for dynamic systems such as the movement of Li in lithium-ion batteries [Ceccio et al. 2020a] [Ceccio et al. 2020b] [Linsenmann et al. 2020] [Nagpure et al. 2014] [Tomandl et al. 2020].

### 3.2.1.3 Requirements

Infrastructure requirements for an NDP instrument are minimal, only requiring basic utilities such as electrical power, internet, and chilled process water (for pump cooling). A beam shutter, beam stop, shielding, benchtop space for experiment preparation, and other equipment would also be needed.

#### **3.2.1.4 Cost and Timeline Estimate**

Design, procurement, assembly, and commissioning of an NDP instrument is expected to cost approximately \$1.0–1.5M. Equipment purchases are estimated to make up 30% of the total budget, with most of the cost allocated to design optimization and instrument installation. Project duration is expected to be 18–24 months. Most of the components for the NDP instrument are commercially available, with the only custom component being the large vacuum chamber.

#### **3.2.2 PGAA and Prompt Gamma Imaging**

The ability to nondestructively evaluate the composition of materials down to the microgram is a critical tool for many technical fields. PGAA is a well-established nondestructive analytical technique that is used to quantify elemental or isotopic concentrations in a wide variety of materials. The technique uses a high flux beam of thermal or cold neutrons to impinge upon a sample, typically mounted in air, and one or multiple high-purity germanium (HPGe) detectors to measure prompt gamma rays emitted from the sample. Radiative neutron capture reactions occur in each isotope of every element with the sole exception of  $^4\text{He}$ , and in theory, PGAA can perform a complete isotopic analysis of almost any material. PGAA is widely used around the world at thermal and cold neutron beam facilities, with approximately a dozen facilities currently in operation. Expanding this capability to HFIR would provide researchers with the tools to perform world-class research in medicine, materials science, geology, archaeology, biology, physics, and many other disciplines. Prompt gamma imaging (PGI), an enhancement of a PGAA instrument, uses programable motor control to move a sample across the neutron beam, providing a rasterized compositional image of the sample. This capability could easily be incorporated into a PGAA instrument with a small cost increase.

The experimental footprint required for a PGAA/PGI facility on a thermal or cold neutron beamline is relatively small. Essential equipment includes a mechanism for holding samples (which are typically small but can be up to several inches in diameter), an HPGe detector with background shielding and Compton suppression, and a small electronics rack for powering and controlling instrument equipment. Equipment necessary for operating the neutron beam line is also required, including a beam collimator or neutron lens to shape the beam, a beam monitor, a beam shutter, a beam stop, and biological shielding. More advanced PGAA instrument designs may include multiple HPGe detectors for coincidence counting and increased detection efficiency, stepper motors for performing PGAA/PGI scans of large samples, sample shielding for analyzing radioactive samples, or complementary analysis instruments such as neutron imaging equipment. A schematic of the PGAA facility proposed for HFIR is shown below in Figure 6.

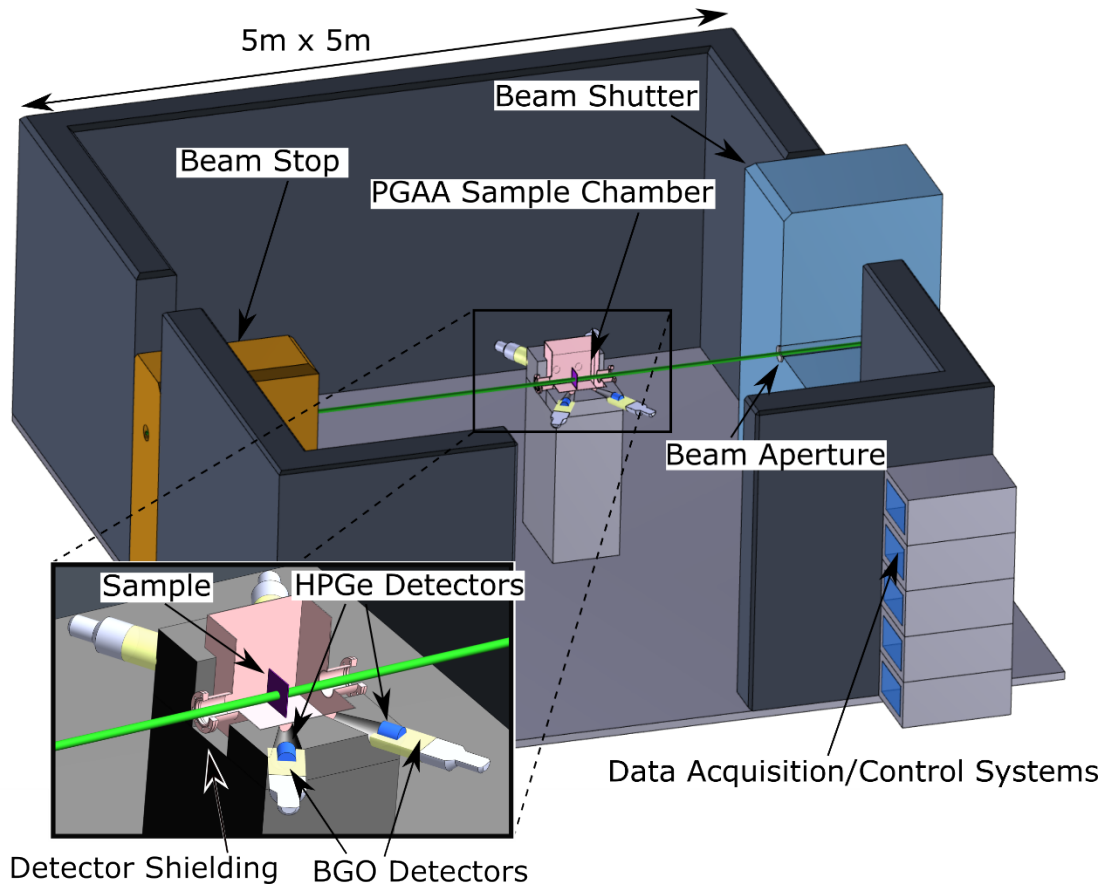


Figure 6. Conceptual design of a PGAA facility on a HFIR beamline.

### 3.2.2.1 Benefits of a PGAA Facility

PGAA is widely used around the world in a multitude of scientific fields. The 2005 Handbook of PGAA [Landsberger 2005] provides an excellent description of the technique and applications with hundreds of references to studies that were performed using PGAA. The 2017 Lindstrom paper [Lindstrom and Révay 2017] provides a more recent review of PGAA and describes new instruments installed in the last 10 years in Argentina, Brazil, China, India, Japan, as well as US university facilities at Oregon State and the University of Texas. More established PGAA facilities in Budapest [Belgya 2012] [Szentmiklósi et al. 2016], and at the National Institute of Standard and Technology in Maryland [Paul et al. 2015] have led to breakthroughs in the last 5 years in archaeological research [Maróti et al. 2020] [Livingston et al. 2018] [Jwa et al. 2018] [Kluge et al. 2018], materials science [Otsuki et al. 2019] [Miura and Matsue 2016] [Artnak et al. 2018], food science [Fukushima et al. 2014], and energy research [Stieghorst et al. 2018].

The true benefit of the PGAA technique is its versatility in the range of samples it can analyze and the minimal sample preparation required. PGAA can be used to analyze samples in solid, liquid, gaseous, or powdered states and does not require dissolution or ablation for analysis. It can also be used to measure very small (mg) or very large (kg) objects if it is equipped with the appropriate mechanical stages. Currently there are no prompt gamma analytical techniques available at HFIR or the Spallation Neutron Source (SNS). Establishing PGAA at HFIR would add new capabilities to one of the highest neutron flux beamlines in the world and would provide a new nondestructive analytical technique to ORNL researchers. Potential programmatic benefits include nondestructive assays for nonproliferation or nuclear forensics, evaluation of fission product assay for nuclear fuels development, measurement of hydrogen

embrittlement in fusion first wall materials, and cross section measurements for rare or short-lived isotopes produced at ORNL.

#### **3.2.2.2 Requirements**

Infrastructure requirements for a PGAA/PGI instrument are minimal: basic utilities such as electrical power, internet, and liquid nitrogen for detector cooling. Additional requirements include a beam shutter, beam stop, shielding, and benchtop space for experiment preparation. Slightly more shielding may be necessary to limit personnel dose rates from the large number of prompt gamma emissions and to suppress background signals in the instrument.

#### **3.2.2.3 Cost and Timeline Estimate**

Design, procurement, assembly, and commissioning of a PGAA/PGI instrument is expected to cost approximately \$1.5–2.0M, most of which would be for instrument design, with significant modeling required to optimize detection efficiency and background suppression. Instrument installation will also require significant personnel time, and the total project duration is expected to require 18–24 months of effort.

### **3.3 SHIELDED DETECTION INSTRUMENTS**

The shielded detection instruments include new detection systems that would be installed outside of the reactor vessel and pool area, making use of the existing assets at HFIR such as the fast neutron flux and the rabbit experimental transfer system. This concept is focused around a new decay station at HFIR which would provide enhanced capabilities in an easily configurable user facility.

#### **3.3.1 The HFIR Decay Station (HDS)**

The HFIR Decay Station (HDS) will be a world-class user and service facility deploying state-of-the-art detector technology capable of complete, correlated spectroscopy with ultra-sensitivity to weak radiation signatures. The concept is to provide a large, granular, high-resolution array of gamma-ray, neutron, and ancillary detectors on a neutron beamline with a fast rabbit connection in an area that can easily be reconfigured to meet an array of experimental needs. Such a facility will serve a wide range of missions, ranging from fundamental nuclear physics experiments to obtain data on nuclear structure or fission dynamics to very applied work such as post-irradiation examination of reactor fuel cladding or development of detectors for use in nuclear safeguards activities. A goal of the HDS will be to provide a single facility capable of taking projects from basic science up through field-ready applications with high technology readiness levels (TRLs). The HDS will serve as a space for basic science and applied experts to converge, paving the way for cross-cutting initiatives and multi-disciplinary innovation across ORNL's core missions to enhance the scientific basis for nuclear technology, to deliver science and technology to address pressing nuclear security challenges, and to design next-generation materials for energy.

Combining the HDS with the proposed On-Line Isotope Facility (OLIF), discussed in greater detail in the HFIR Futures – Enhanced Capabilities Series Volume 12: Flow Loop Facilities (ORNL/TM-2022/2691/V12), will push the envelope even further, making the HDS a one-of-a-kind world center for fundamental nuclear physics and applied nuclear engineering. The OLIF will supply small, purified samples of short- or long-lived radioactive isotopes and rare actinides directly to the detector array. Combining the HDS and OLIF with a neutron beam line, rabbit system, and neighboring Radiochemical Engineering Development Center (REDC) would be highly agile, broad in capability, and entirely unique.

A large, granular, high-resolution array like the HDS is significantly more sensitive to weak decay signatures than a single HPGe detector because of its ability to perform time- and energy-correlated coincidence measurements to effectively suppress the background and provide selectivity to specific decay channels or isotopes. This technique is common to basic research in nuclear physics, but it has not yet penetrated the application space. Coincidences offer significant advantages for measurement of precise absolute decay branching ratios or identification and quantification of specific isotopes / materials, particularly for cases in which the radiation signature is weak or obscured by significant background radiation. This technique is powerful enough to isolate a single transition in a rotational band of a single fission product from a sample of fissile material [Fernández and Victoria 2019]. A stated goal of the HDS is to make these advanced spectroscopic techniques available to a much wider user base, enabling innovation within fields such as nuclear forensics, nuclear safeguards, reactor fuel development, and beyond.

An example of the coincidence technique is shown in Figure 7, with data from the CLARION Compton-suppressed HPGe detector array. This array was previously located at ORNL’s DOE Nuclear Physics Holifield Radioactive Ion Beam Facility (HRIBF). A thin natural silver foil was irradiated at HFIR [Gross et al. 2000] and was subsequently counted for discovery of “forbidden” transitions as a precision test of the vibrational model. The top histogram shows a traditional measurement of the radiation from the foil, usually referred to as a *singles measurement*, with the entire CLARION detector. This type of singles measurement is the standard method in most application spaces. The bottom histogram shows coincidence data from  $^{110}\text{Cd}$  following the beta decay of  $^{110\text{m}}\text{Ag}$  that was extracted by looking for gamma rays in coincidence with a 1783-keV gamma ray (a previously known transition in  $^{110}\text{Cd}$ ). Many of the observed weak transitions—decay branches of 1 in 200,000 beta decays of  $^{110\text{m}}\text{Ag}$  [Allmond 2016]—were otherwise inaccessible in the top histogram.

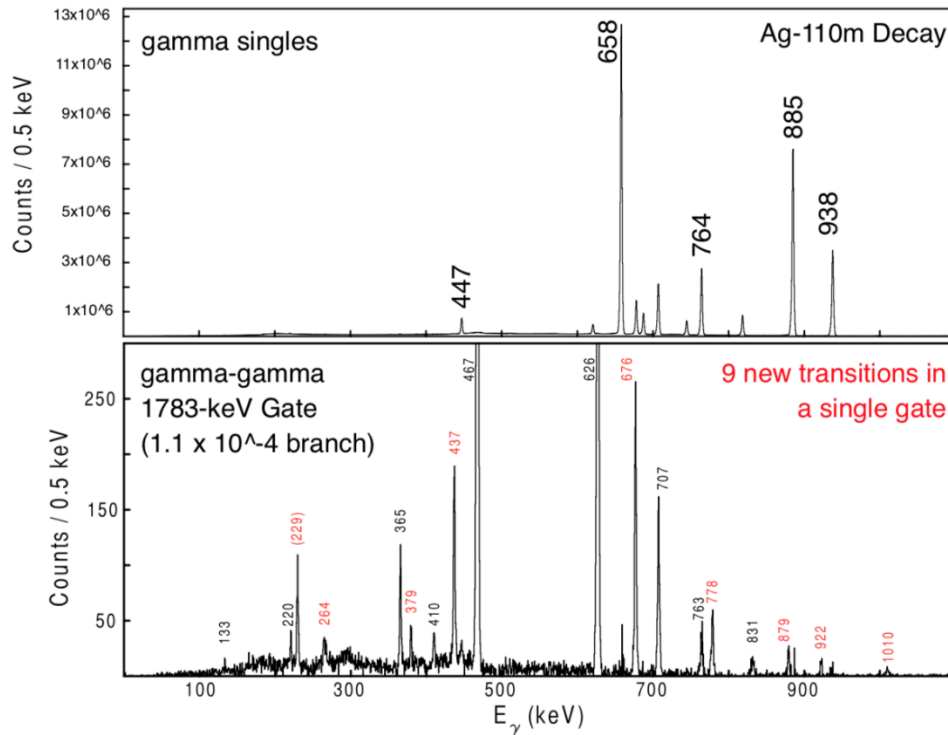


**Figure 7.** Two histograms showing a measurement with the CLARION detector of a silver foil that was irradiated within HFIR [Gross et al. 2000]: (top) measurement of radiation being emitted by the silver foil without any coincidences in place; desired transition not visible in this spectrum; (bottom) coincidence gate placed on a 1783-keV gamma ray emitted by  $^{110}\text{Cd}$  after  $^{110\text{m}}\text{Ag}$  beta decay. This gate revealed 9 previously unknown

transitions in  $^{110}\text{Cd}$  [Allmond 2016], thus demonstrating the selectivity of the technique and its ability to suppress background.

The coincidence technique can be applied more generally to gamma-gamma, beta-gamma, alpha-gamma, fission-gamma, fission-beta-gamma, fission-beta-gamma-neutron measurements, and more, thus improving the signal-to-noise ratio and eliminating the need for separate background counting and subsequent subtraction.

### 3.3.2 Precision Frontier of Science and Applications Enabled by the HDS

The HDS will enable precision-frontier activities across divisions and directorates on topics such as fundamental nuclear physics, forensics, safeguards, medicine, materials science, archaeology, biology, and geology. By paring the HDS with other ORNL capabilities, such as the Neutron Beam Line, the Fast Rabbit, REDC, and OLIF, the opportunities can be collectively maximized, as shown in Figure 8. A few examples are as follows:

- Fission electron yield integrals for reactor neutrino anomaly
- PGAA
- Ultra-sensitive material identification, radiation localization (imaging), and quantification for forensics
- Detection science and safeguards – radiation signature discovery
- Neutron cross section measurements
- Transmutation vs. burnup cross sections of actinides
- Prompt fission-induced gamma ray emission
- Correlated event-by-event fission dynamics of common and exotic actinides
- Nuclear reactions such as two-neutron pickup on  $(n, ^3\text{He})$  for pairing correlations
- Fission product distributions
- Isomer creation with pulsed neutron beam
- Neutron irradiation/activation effects on materials and electronics
- Correlation of triaxial deformation of n-rich nuclei with inertial dynamics, masses, moments, charge-radii, and r-process nucleosynthesis
- Search for cross-shell excitations, single-particle fragmentation, and shape coexistence of n-rich nuclei near or beyond double-magic  $^{132}\text{Sn}$  and  $^{78}\text{Ni}$
- Quantification of nucleon-nucleon correlations and role of the p-n interaction in driving nuclear deformation

- Beta, gamma, and neutron spectra shapes of n-rich nuclei for decay heat / reactor design, fundamental science, and nuclear forensics
- Post-irradiation examination of materials and reactor fuel

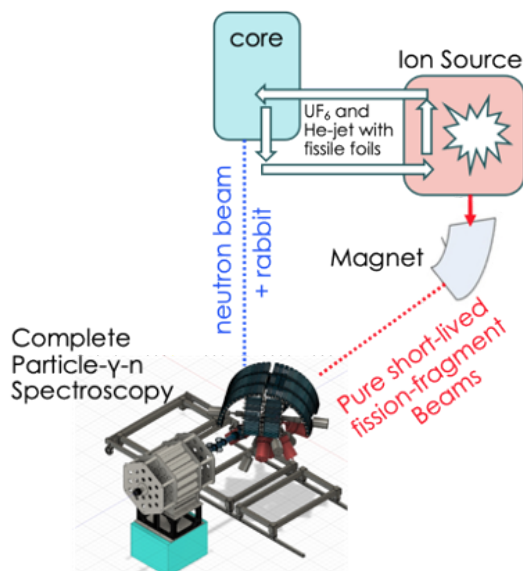


Figure 8. HDS within a wider context of ORNL capabilities.

### 3.3.3 Preliminary Design and Configuration Concepts of the HDS

The design concept for the HDS—similar to the FRIB Decay Station initiator (FDS) led by ORNL and the University of Tennessee, Knoxville (UTK) [Savard et al. 2015]—is to establish a detector room with an integrated and reconfigurable suite of gamma-ray, neutron, and charged particle detectors for discrete (differential) and total absorption (integral) spectroscopy. Providing a complement of integrated and reconfigurable frames plus detectors will allow HDS staff to easily prepare various detector configurations to best meet the needs of a given experiment. Preconceptual designs and configurations are shown in Figure 9.

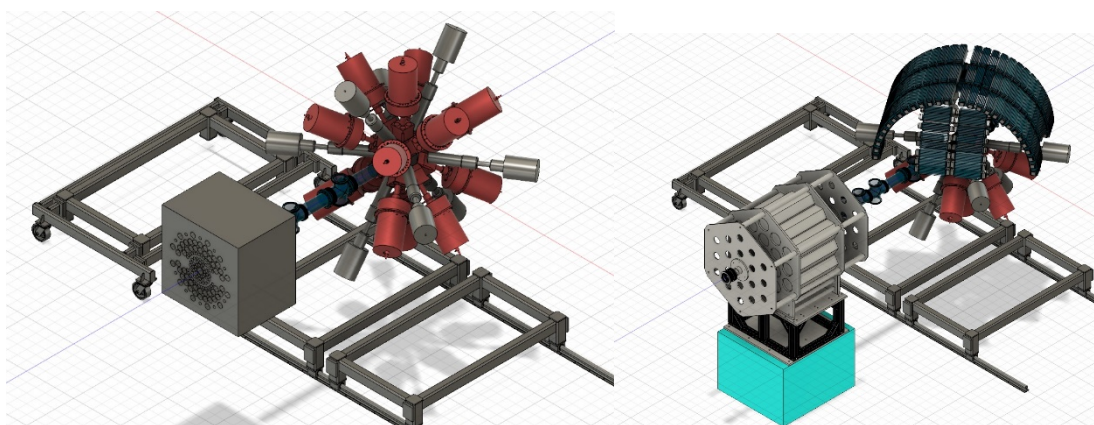


Figure 9. Preconceptual HDS designs and configurations for enabling complete spectroscopy of gamma, neutron, and charged-particle radiation with ultra-sensitivity to weak decay signatures.



The HDS will include a suite of inner chambers and sample holders to be placed inside the array for various configurations. These will be integrated with (1) charged particle detectors, useful for any experiment to study alpha or beta emitting nuclides, (2) an interlock for the fast rabbit system, and (3) a rotating collimator for neutron and gamma ray imaging and localization. The chambers can be designed to work under vacuum, in air, or with inert gas, and they may also serve to heat or cool the enclosed samples.

Smaller funding sources, including seed funding and LDRD efforts, could be pursued separately to rapidly expand HDS experimental capabilities through the creation of additional auxiliary chambers and detectors.

### 3.3.4 ORNL Expertise and Leadership on HDS-Style Arrays

ORNL has significant demonstrated expertise in developing HDS-style arrays for the DOE-NP mission, particularly in the context of RIB user facilities [Cloet and Kay 2020] [Savard et al. 2015] [Borge and Riisager 2016]. However, none of these arrays or facilities, which primarily target fundamental science inquiries, are located at ORNL. Two recent examples include (1) CLARION2-TRINITY [Gray et al. 2022] at Florida State University (FSU), which will eventually move to the FRIB, and (2) the FRIB Decay Station initiator (FDSi) [Cloet and Kay 2020], which will remain at FRIB. Experience with the development of these arrays can be leveraged with the HFIR upgrade to build a state-of-the-art radiation detector and a facility for the conduct of cross-cutting fundamental science and applications missions at ORNL.

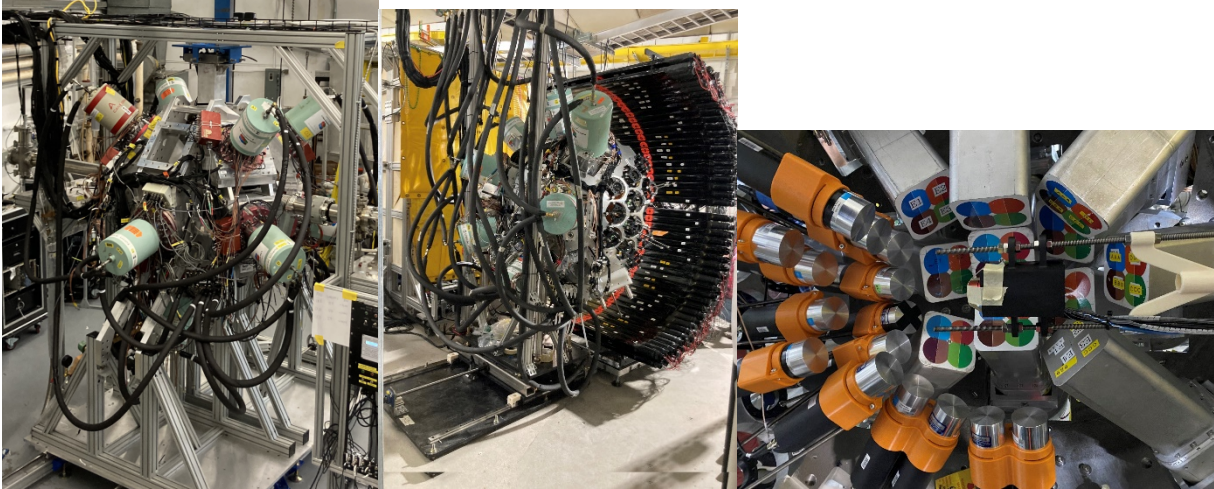


**Figure 10. Recent HDS-style arrays (but previous generation) built and led by ORNL: (left) CLARION2-TRINITY [Gray et al. 2022] at the FSU John D. Fox Laboratory, (middle) FDSi [n.d.] at FRIB, and (right) FDSi interior [FDSi n.d.].**

### 3.3.5 Comparison of HDS with Similar Arrays and Facilities

The Fission Product Prompt Gamma-ray Spectrometer (FIPPS) array, located at the Institut Laue-Langevin (ILL) High-Flux Reactor in France (i.e., FIPPS at ILL) [Blanc et al. 2013], is the HDS at HFIR's most direct competitor.

FIPPS phase 1 has an efficiency of 4% at 1.3 MeV and is on a neutron beam with a flux of  $10^8$  n/cm<sup>2</sup>/s [Blanc et al. 2013]. As proposed, the HDS will be ~22% efficient at 1.3 MeV and will be located on a neutron beam with a flux of  $\sim 10^{10}$  n/cm<sup>2</sup>/s. Detection efficiency is vitally important in detector arrays

because it is the determining factor of measurement sensitivity, and coincidence measurements multiply these efficiencies. When combined with the higher neutron flux, the HDS at HFIR will be three or more orders of magnitude more sensitive to weak decay signatures than FIPPS at ILL. The efficiencies of HPGe arrays within North America are shown in Figure 11 for comparison. The red DEGA line represents the expected gamma-ray efficiency of the HDS.

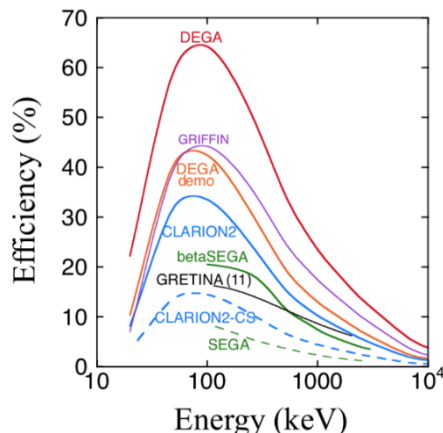


**Figure 11. Gamma-ray detection efficiencies of HPGe arrays in North America: DEGA-HDS is the top red line with the highest efficiency.**

No facility in the world combines a radioactive isotope production facility, neutron beam line, fast rabbit, and neighboring REDC. *The HDS at HFIR will have capabilities that are unmatched by any other facility world-wide.*

### 3.3.6 HDS Footprint, Requirements, and Possible Locations

The array will require a large amount of space to accommodate different detector configurations and shielding: the HDS footprint will be approximately  $5 \times 5$  m. Temporary access outside this footprint will be required to reconfigure the array. Large doors, crane/lifting access, and storage space will also be needed.

To fully compete with the neutron flux available at the FIPPS detector at ILL, an experimental location with a neutron flux of  $\geq 10^8$  n/cm<sup>2</sup>/s is required, but preferably approximately  $10^{10}$  n/cm<sup>2</sup>/s [Blanc et al. 2013]. The HDS should be shielded from strong magnets, the reactor core, and any radiation background-inducing equipment or storage.

A few possible locations might meet these requirements; the preferred location is at the end of the Cold Neutron Guide Hall because it provides a neutron flux of approximately  $10^{10}$  n/cm<sup>2</sup>/s, which is more than sufficient for HDS needs. If the back wall of the guide hall could be extended, or if a room could be added in the back, then this location would be ideal. Two other possible locations are in the HB2 measurement hall or in the planned new guide hall.

### 3.3.7 HDS Operations and Access

A Technical Advisory Committee and a Users Executive Committee will be established for HDS. The Users Executive Committee will host a yearly town hall to foster collaboration between applied and fundamental nuclear experts.

The HDS will serve as a user and service facility. Other facilities with similar arrays require proposals with subsequent Project Approval Committee (PAC) approval. Once the PAC approves a proposal based on scientific merit, or once access to the device is granted, the user must perform the experiment and analyze the results. A student or postdoc is typically responsible for the analysis, which can take 1–2 years for results. Datasets typically range from GB to many TB in size, requiring specialized codes for each experiment to scan, correlate, and visualize the results. Whereas the HDS will continue to support this research mode of operation with customized / changing configurations and software for highly specialized users, it will also operate as a service with well-calibrated nominal configurations and software for rapid turnaround of results to non-expert staff and customers. Full-time instrument scientists, data analysts, and environmental specialists will be required to achieve these services, placing access to the world's most sensitive radiation detector in the hands of nontraditional users for the first time. This service will provide the customer with an ultrasensitive nondestructive isotopic analysis of materials beyond anything possible today.

### **3.3.8 HDS Cost and Schedule Profile**

The total estimated cost range of the HDS is \$24–30M (omitting ORNL labor and overhead), which is based on a combination of budgetary quotes and actual costs from prior projects. The time required to design and build the entire HDS is 5–8 years.

## **3.4 ULTRACOLD NEUTRON SOURCE**

Fundamental neutron physicists use the neutron to address some of the most compelling science questions in nuclear and particle physics, astrophysics, and cosmology. Measurements of the properties of the neutron and its interactions are used to develop a more complete understanding of the fundamental forces of nature and the nature of matter in the universe. A world-leading program of fundamental neutron physics research has been developed using cold neutrons at the SNS. Achievements include the first observation of the weak interaction between the neutron and the proton, the first measurement of the parity violating asymmetry in the neutron- $^3\text{He}$  weak interaction, and an experiment which ruled out mirror neutron oscillations as an explanation of the neutron lifetime puzzle—the long-standing disagreement between cold neutron beam and ultracold neutron (UCN) bottle measurements. Over the next decade, the current Neutron  $\alpha$  b (Nab) experiment at SNS will be used to study neutron beta decay with unprecedented precision to gain new understanding of this phenomenon—a potential area of new physics. Meanwhile, the world's most ambitious search for the neutron electric dipole moment (nEDM) will be installed and commissioned following Nab. The search for the nEDM is one of the most compelling experimental pursuits in nuclear physics to gain an understanding of the lack of antimatter in the universe.

These advances will not only require developments in experimental technology, but also substantial increases in the neutron intensity available for experiments. The planned upgrade of the HFIR pressure vessel creates an especially rare opportunity. By including considerations in the design of the new pressure vessel, the development of a world-leading source of ultracold neutrons becomes possible with the potential to provide density two or three orders of magnitude higher than from currently available neutron sources. Such a facility would give rise to a new, diverse class of experiments at ORNL, ranging from studies of beta decay, exotic interactions, and gravitational states. Materials science could also take advantage of such a source of neutrons, with new applications in imaging and the ability to measure the heat capacity of a monolayer of material. These upgraded facilities represent an excellent opportunity to build on SNS success and to further ORNL's world-leading fundamental physics program.

### 3.4.1 Overview of Current Ultracold Neutron Sources

This section presents a brief overview of existing reactor based UCN sources. Operating and planned spallation UCN sources are not discussed here. The goal of the overview is to present the current state of reactor UCN sources and to develop an idea of the neutron fluxes required to develop a UCN source. These fluxes must then be compared with HFIR's fluxes, and subsequent conclusions must be drawn regarding the potential of a UCN source at HFIR.

UCN sources from a reactor are generated by slowing thermal neutrons having speeds of  $2.2 \text{ km.s}^{-1}$  down to speeds of less than  $8 \text{ m.s}^{-1}$ . This is accomplished by impinging the thermal neutrons on a multistage neutron moderator, which is collectively known as the *converter*. The thermal neutron flux can therefore be regarded as a measure of the potential of generating UCNs. However, the actual performance of the UCN source is more complicated and depends on many physics and engineering considerations, including moderator selection and physical configuration, and moderator coolability. Once generated, the UCNs can be collected and stored in bottles for use in experiments, or they can be used to create a UCN beam which is used in irradiation experiments. In the case of neutron storage, the density of UCNs,  $\text{UCN.cm}^{-3}$ , is a measure of performance, whereas in the case of a UCN beam, the neutron flux,  $\text{UCN.cm}^{-2}.\text{s}^{-1}$ , is the measure of system performance.

In this discussion, UCN density and flux are used as measures of UCN source performance. The level of thermal neutron flux is used as an indicator for UCN generation potential. The actual quantity of importance is the total number of neutrons that impinge the converter over a given surface area, but because the details of various designs are unknown (e.g., exact fluxes and surface areas to convert a flux [ $\text{n.cm}^{-2}.\text{s}^{-1}$ ] to a current [ $\text{n.s}^{-1}$ ]), the thermal flux level is used as a measure.

Table 2 lists current operational reactor UCN sources and sources under construction. The present operational sources are in France (ILL) and Germany (TRIGA Mainz and FRM II). ILL currently produces the highest density at a reactor power of 58 MW and between  $36\text{--}55 \text{ UCN.cm}^{-3}$  (depending on the converter), with a thermal flux of  $2.5\text{E}14 \text{ n.cm}^{-2}.\text{s}^{-1}$ . When pulsed at 250 MW an estimated thermal flux of  $7\text{E}13 \text{ n.cm}^{-2}.\text{s}^{-1}$  TRIGA Mainz can produce  $8.5 \text{ UCN.cm}^{-3}$ . In the United States, the UCN source at North Carolina State University is presently in the testing phase.

Using the thermal neutron flux as a measure of UCN potential, thermal fluxes between  $1\text{E}12$  and  $2.4\text{E}14 \text{ n.cm}^{-2}.\text{s}^{-1}$  (along with the appropriate converter) can generate UCN neutrons. In general, the higher the flux, the greater the potential; however, the cases of PIK and WWR-M illustrate the point regarding the importance of neutron current mentioned above. That is, WWR-M, with a lower thermal flux of  $3\text{E}12 \text{ n.cm}^{-2}.\text{s}^{-1}$ , can produce as much UCNs at PIK with a higher thermal flux of  $2.4\text{E}14 \text{ n.cm}^{-2}.\text{s}^{-1}$ . The reason for this can be understood by considering the conceptual designs for WWR-M and PIK in Figure 12 and Figure 13, respectively. In the case of WWR-M, a low flux is collected close to the core over a 1 m diameter cylindrical area into a thermal column. In the PIK, the UCN sources are on beam tubes GEK-3 and GEK-4 and are collected over tubes with much smaller diameters. Therefore, the usable number of neutrons in the WWR-M UCN source (neutron current) is likely the same as that of PIK.

Scientific research requires greater neutron UCN densities and fluxes, which has led to research and development of superfluid helium (a quantum fluid) as the final stage of the UCN converter. This development occurred over a period of 20 years through collaborations at ILL at the Petersburg Nuclear Physics Institute (PNPI) in Russia **Error! Reference source not found..** The most advanced UCN sources based on superfluid helium are being developed at the PIK and WWR-M reactors, which are operating at 100 MW ( $2.4\text{E}14 \text{ n.cm}^{-2}.\text{s}^{-1}$ ) and 18 MW ( $3\text{E}12 \text{ n.cm}^{-2}.\text{s}^{-1}$ ), respectively. The designed UCN source density for PIK is  $13,000 \text{ UCN.cm}^{-3}$ , and it is between 840 and  $13,000 \text{ cm}^{-3}$  for WWR-M, setting the stage for advanced physics research.



**Table 2. Comparison of operating and planned UCN sources**

Reactor	Organization	Reactor power and moderator	UCN converter	Estimated operational thermal flux [n.cm <sup>-2</sup> .s <sup>-1</sup> ]	UCN source	Operational status
ILL (PF2) High Flux Reactor <b>Error! Reference source not found. Error! Reference source not found. Error! Reference source not found.</b>	Institute Laue-Langevin, Grenoble, France	<b>58 MW</b> Heavy water	Solid deuterium	<b>2.5E+14</b> in source region	Density: <b>36</b> UCN.cm <sup>-3</sup> Flux: <b>3.3E+04</b> UCN.cm <sup>-2</sup> .s <sup>-1</sup>	Operational
			Superfluid helium		Density: <b>55</b> UCN.cm <sup>-3</sup>	Operational
TRIGA Mainz <b>Error! Reference source not found.</b>	Johannes Gutenberg University, Mainz, Germany	<b>Pulsed 250 MW</b> Graphite/water	Solid deuterium	<b>7E+13</b> in the thermal column	Density: <b>8.5</b> UCN.cm <sup>-3</sup>	Operational
PULSTAR <b>Error! Reference source not found.</b>	North Carolina State University, United States	<b>1 MW</b> full power operation	Heavy water and solid methane	<b>1E+12</b> at entrance to heavy water tank	Estimated production rate in methane: 8000-15,000 UCN.cm <sup>-3</sup> .s <sup>-1</sup> *Note this is before collection of usable UCN flux or density.	Testing
FRM II <b>Error! Reference source not found. Error! Reference source not found.] Error! Reference source not found. Error! Reference source not found.</b>	Technical University Munich, Germany	<b>20 MW</b> , Heavy water	Solid deuterium	<b>*8E14</b> in moderator region NOT on source	Designed flux: 6E+05 UCN.cm <sup>-2</sup> .s <sup>-1</sup>	Under construction
PIK <b>Error! Reference source not found. Error! Reference source not found.</b>	Petersburg Nuclear Physics Institute, Russia	<b>100MW</b> , Light water and heavy water reflector	Liquid deuterium and superfluid helium	<b>2.4E+14</b> in beam tubes GEK-3 and GEK-4	Designed density: <b>13,000</b> UCN.cm <sup>-3</sup>	Under construction

<b>Error! Reference source not found. Error! Reference source not found.</b>						
WWR-M <b>Error! Reference source not found. Error! Reference source not found. Error! Reference source not found. Error! Reference source not found. Error! Reference source not found. Error! Reference source not found. Error! Reference source not found.</b>	Petersburg Nuclear Physics Institute, Russia	<b>18 MW,</b> Beryllium and light water	Liquid deuterium and superfluid helium	<b>3E+12 in the source region</b>	Designed density: <b>840–13,000</b> cm <sup>-3</sup>	Under construction

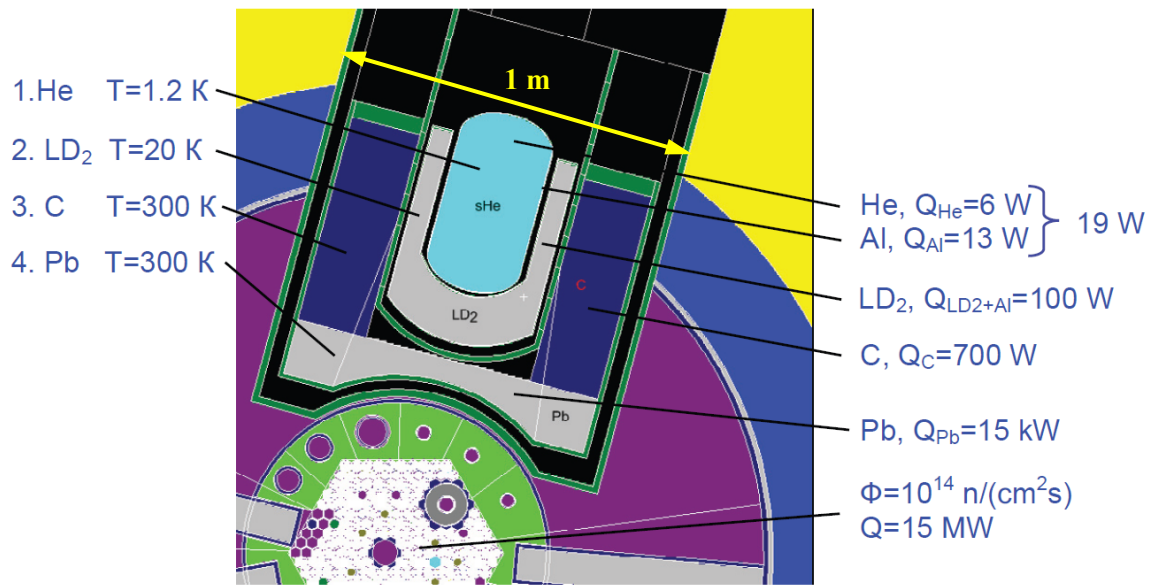


Figure 12. WWR-M thermal column UCN source design (large collection of low flux in thermal column) Error! Reference source not found..

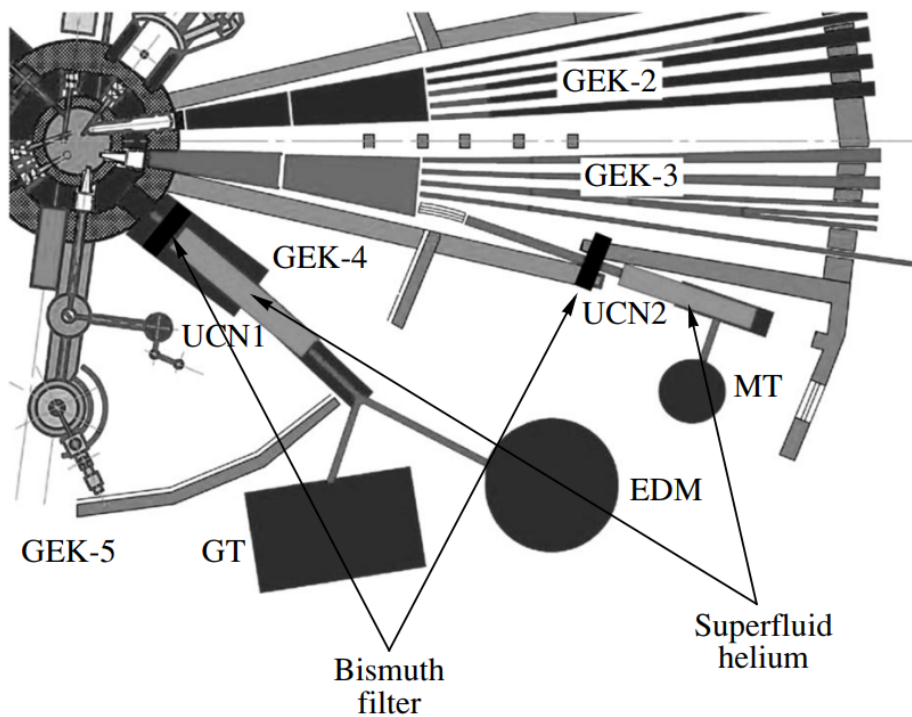


Figure 13. PIK beam tube UCN source design (low collection of flux in small GEK-3 and GEK-4 tubes) Error! Reference source not found..



### 3.4.2 Neutron Fluxes on HFIR Beam Tubes

A thermal neutron flux map was calculated for HFIR to determine the potential for installing a UCN source on one of the HB beam lines. Figure 14 shows the thermal neutron ( $E < 0.025$  eV) over a 5 cm high horizontal slice through the core center line and over a core area of approximately  $1 \times 1$  m. The inset in the lower right corner of the figure shows the Monte Carlo N-Particle (MCNP) model, along with the HB beam lines.

The thermal fluxes in the beam tubes range from  $1\text{E}+12 - 1.5\text{E}14$  n.  $\text{cm}^{-2}.\text{s}^{-1}$ . Therefore, the HFIR thermal flux levels are in the range of the required fluxes given in Table 2:  $3\text{E}12 - 2.5\text{E}14$  n.  $\text{cm}^{-2}.\text{s}^{-1}$ , although they are not quite as high as ILL and the PIK fluxes. However, the initial indication is that a UCN source is a viable option in one of the HB beam tubes.

To utilize the flux of  $1.5\text{E}14$  n.  $\text{cm}^{-2}.\text{s}^{-1}$  in HFIR, the UCN converter must be installed closer to the core if the existing diameter beam tubes are used. Making use of a lower flux level further away from the core would likely require an increase in the beam tube diameter to collect more neutrons into the converter, as in the case of the WWR-M **Error! Reference source not found.** which uses a lower flux level into a large thermal column (see Figure 12).

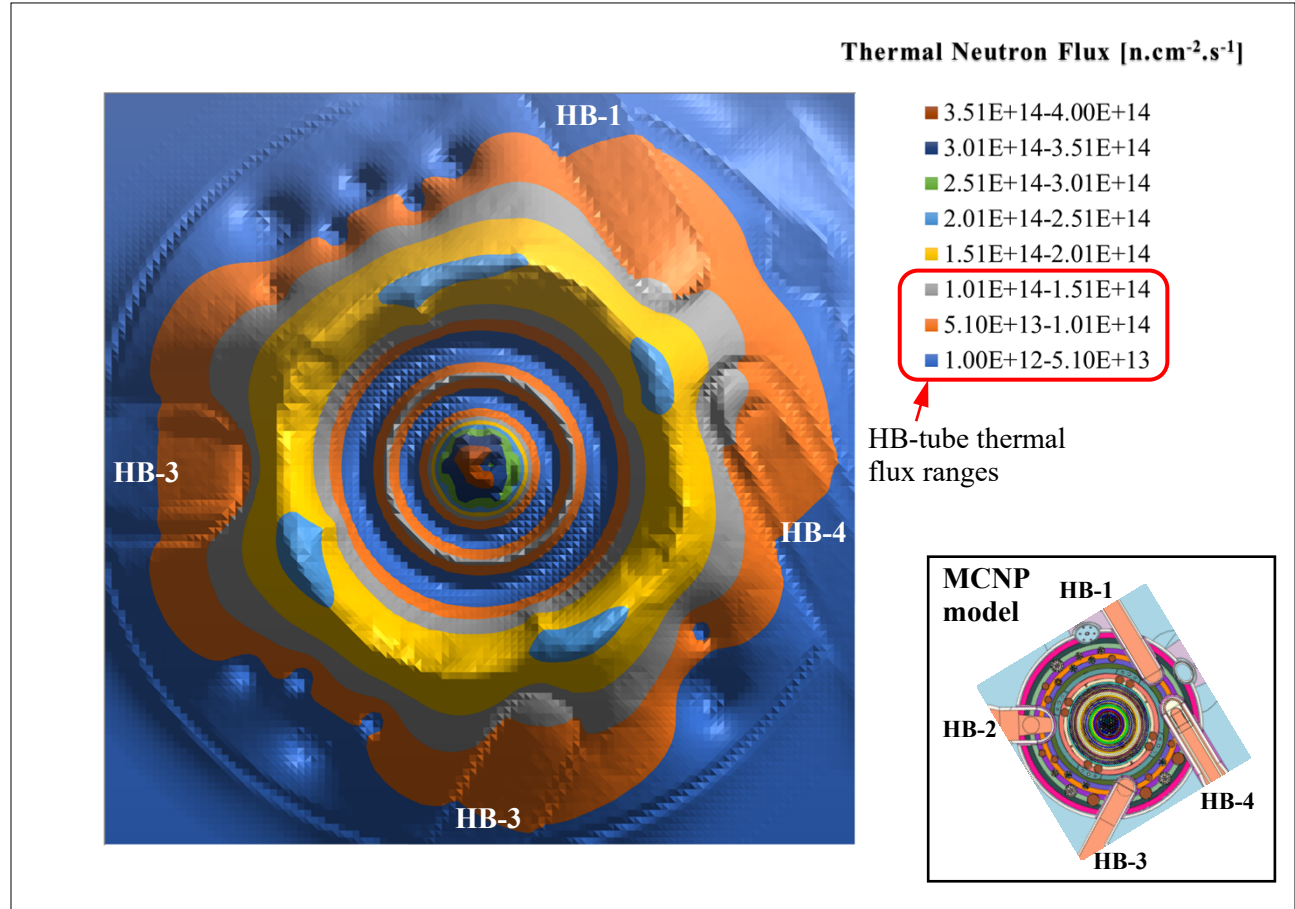


Figure 14. HFIR thermal flux map.

### 3.4.3 Design Requirements

The design requirements for a UCN source depend on its application or the type of intended research for which it will be used. The requirements set forth here are general, with the goal of providing the largest possible UCN density and beam flux to address future physics research needs:

1. The estimated incident thermal neutron current onto the converter is approximately  $1\text{E}14\text{--}1\text{E}16\text{ n.s}^{-1}$ . This estimate was developed (current = flux  $\times$  area) based on the thermal fluxes for WWR-M ( $3.12\text{E}14\text{ n.cm}^{-2}.\text{s}^{-1}$ ) and PIK ( $2.5\text{E}14\text{ n.cm}^{-2}.\text{s}^{-1}$ ) and on the estimates of the thermal column and beam tube diameter information available, respectively.
2. A UCN density of approximately  $13,000\text{ cm}^{-3}$  or greater is required.
3. A UCN flux of  $6\text{E}+05\text{ UCN.cm}^{-2}.\text{s}^{-1}$  or higher is required.
4. To achieve the requirements listed above, a coupled two-stage solid deuterium and superfluid helium must be used.
5. In a broad sense, the UCN source engineering should:
  - a. provide sufficient cooling,
  - b. provide easy system maintenance,
  - c. allow equipment upgrading,
  - d. be able to accommodate different physics experiments, and
  - e. allow for future experiment upgrades.

### 3.4.4 Limitations/Challenges

Based on the literature review of reactor-based UCN sources presented in Section 3.4.1, available thermal neutron fluxes in HFIR, and the scoping analyses presented in Section 3.4.6, it can be concluded that HFIR can accommodate an advanced UCN source using larger beam tubes and with the converter installation as close to the reactor as possible. Some additional design needs are as follows:

1. HFIR will need to be able to accommodate changes in the core structures (reflector and irradiation position) while still maintaining its current range of applications in isotope production and the neutron sciences.
2. The proposed location of the UCN converter is as close to the core as possible, and with superfluid helium, the temperature must be maintained between 1 and 5 K. This proximity to the core will expose the UCN converter to high levels of neutron and gamma irradiation, including exposure to radiation damage and heat. However, these challenges have been addressed at the ILL, PIK, and WWR-M reactors **Error! Reference source not found.**, so any issues that might be faced will be specific to HFIR.

### 3.4.5 Impacts to HFIR

The installation of a UCN source will likely impact the following HFIR systems:

1. beryllium reflector,
2. beam tube penetrations into reactor pressure vessel,
3. irradiation positions (large and small vertical experiment facilities [VXF]) in the reflector,
4. HFIR reactor physics characteristics and cycle length,

5. the size of the penetration through the biological shield,
6. HFIR instrumentation and controls, and
7. likely other systems.

### 3.4.6 Scoping Analyses

To determine whether HFIR meets the thermal neutron current requirement for a UCN source, a series of neutron transport analyses was performed to assess the present neutron flux and the current capabilities for various beam lines. In all cases, the thermal neutron current (in  $\text{n.s}^{-1}$ ) was computed in the outgoing direction of the beam axis, essentially representing the thermal neutron source that would impinge the first stage of the UCN converter. All the analyses were performed with MCNP and with HFIR at 85 MW thermal power.

Neutron currents were calculated on beam tubes HB-1 through HB-4 and EF-1. In addition, conceptual designs with larger diameter tubes on HB-2 and EF-1 were analyzed to investigate the thermal neutron source strength. Impacts to the reactor physics parameters and HFIR cycle lengths caused by changes on the beam line diameters were not considered as part of this study.

#### 3.4.6.1 Neutron Currents on HFIR HB beamlines

Figure 15 presents a horizontal section from the MCNP model of HFIR's core midplane, showing HB-1 to HB-4. All the beamlines extend outward from the core and penetrate the reactor pressure vessel at points indicated by **A**. Entrance to the concrete biological shield (bio-shield) is indicated at points **B**, and exits from the bio-shield are indicated at points **C**. The outgoing thermal neutron currents ( $E < 0.025$  eV) and fluxes were calculated at points A, B and C for each beamline. The results are shown in Table 3 and Figure 16.

The easiest location at which to install a UCN source would be at the beam tube exit at the bio-shield: at any of the points marked C. The highest impinging current would be available on beam HB-2 at  $2\text{E}+12$   $\text{n.s}^{-1}$ , which is two orders of magnitude lower than the minimum desired requirement of  $1\text{E}+14$   $\text{n.s}^{-1}$ . Because HB-2 has a larger tube entrance and is closer to the core, it collects more neutrons which stream down the tube, resulting in a higher impinging current value. The thermal currents on HB-1, HB-3, and HB-4 are lower than that of HB-2 by a factor of 10, likely because the beams tubes are not radially located relative to the core and the smaller beam tube entrances.

In all cases, results indicate that larger beam tubes would be required to collect more thermal neutrons from the core. Alternatively, the converter could be installed closer to the core. Point A of HB-2, which has a thermal current of  $5\text{E}+14$   $\text{n.s}^{-1}$  (flux of  $1\text{E}+12$   $\text{n.cm}^{-2}.\text{s}^{-1}$ ), is a candidate location.

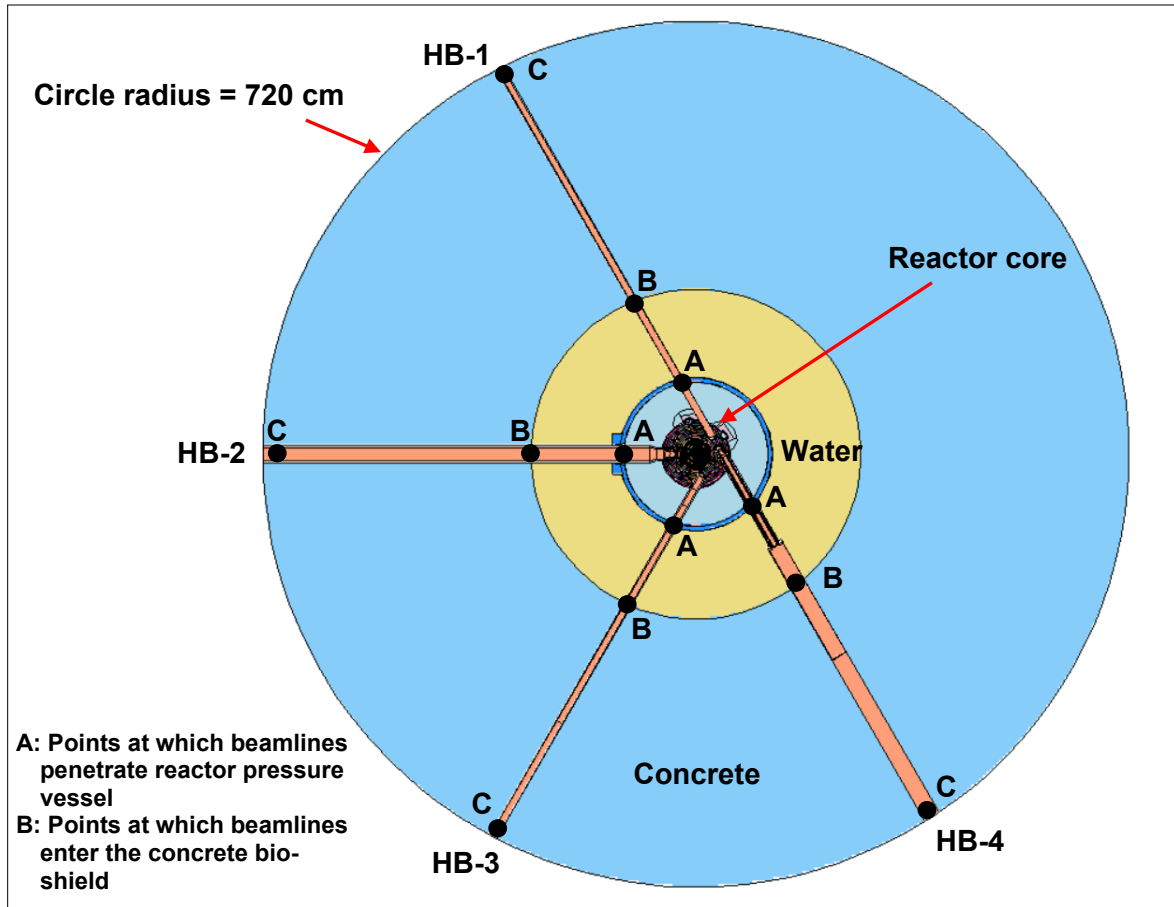


Figure 15. MCNP model showing HFIR beam lines and location types where neutron currents were calculated.

Table 3. HFIR HB beam tube currents and fluxes

Location	Forward thermal neutron current (n.s <sup>-1</sup> )				Estimated forward thermal fluxes (n.cm <sup>-2</sup> .s <sup>-1</sup> ) (Cross sectional area of circular disk perpendicular to beam axis)			
	HB-1	HB-2	HB-3	HB-4	HB-1 (81 cm <sup>2</sup> )	HB-2 (415 cm <sup>2</sup> )	HB-3 (81 cm <sup>2</sup> )	HB-4 (127 cm <sup>2</sup> ) <sup>a</sup> (556 cm <sup>2</sup> ) <sup>b</sup>
A	2E+13	5E+14	3E+13	7E+13	3E+11	1E+12	4E+11	5E+11 <sup>a</sup>
B	1E+12	2E+13	1E+12	8E+12	1E+10	6E+10	2E+10	1E+10 <sup>b</sup>
C	1E+11	2E+12	1E+11	9E+11	2E+09	4E+09	2E+09	2E+09 <sup>b</sup>

<sup>a</sup> = cross-sectional area with a smaller diameter portion of HB-4

<sup>b</sup> = cross-sectional area with a larger diameter portion of HB-4

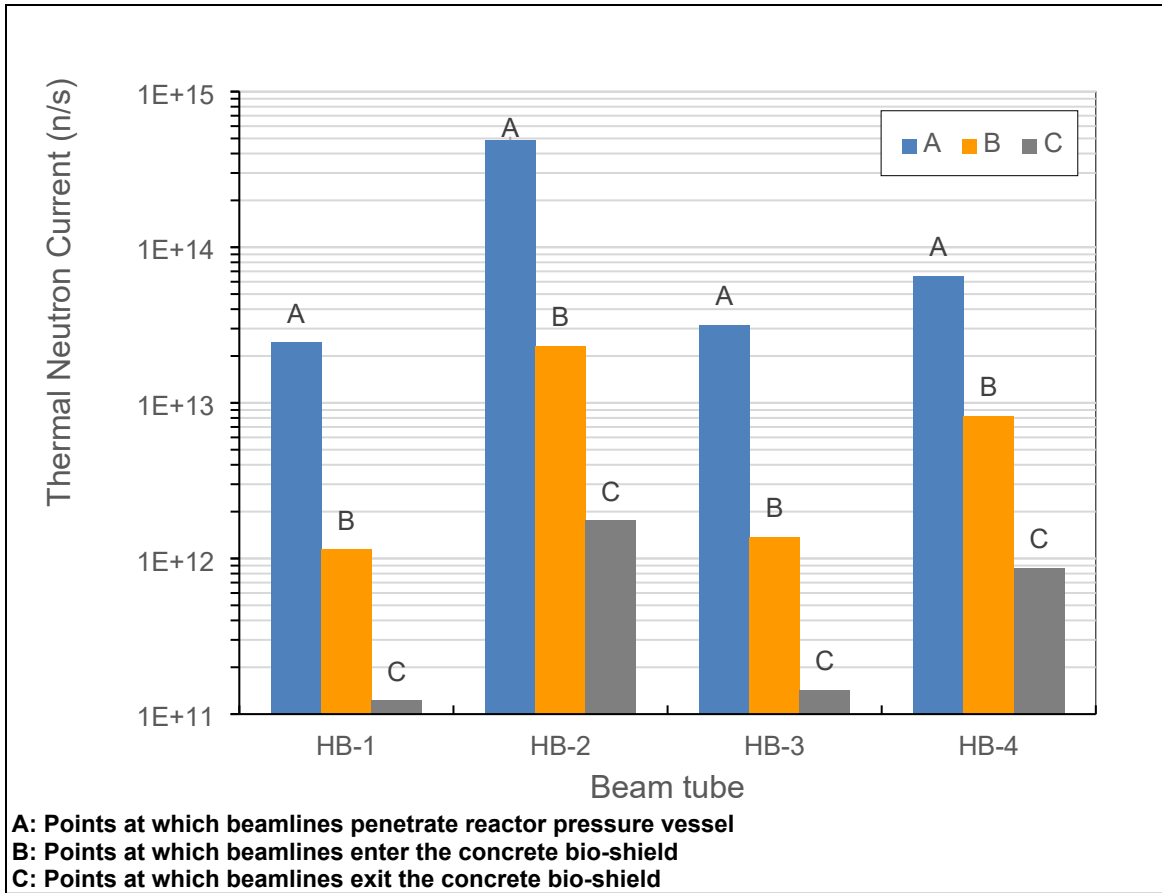


Figure 16. HFIR HB beam tube currents.

### 3.4.6.2 Larger diameter HB-2 tube

Based on the HB tube neutron currents presented in Table 3 and experiences from the WWR-M reactor (low flux and large tube), the neutron current requirement could be met by enlarging the beam tubes. To quantitatively investigate this option, a conceptual design with an enlarged HB-2 tube having an inner diameter of 60 cm was analyzed as shown in Figure 17, and the neutron currents and fluxes were calculated at the same points as those shown in Figure 18. The resulting currents and fluxes are given in Table 4.

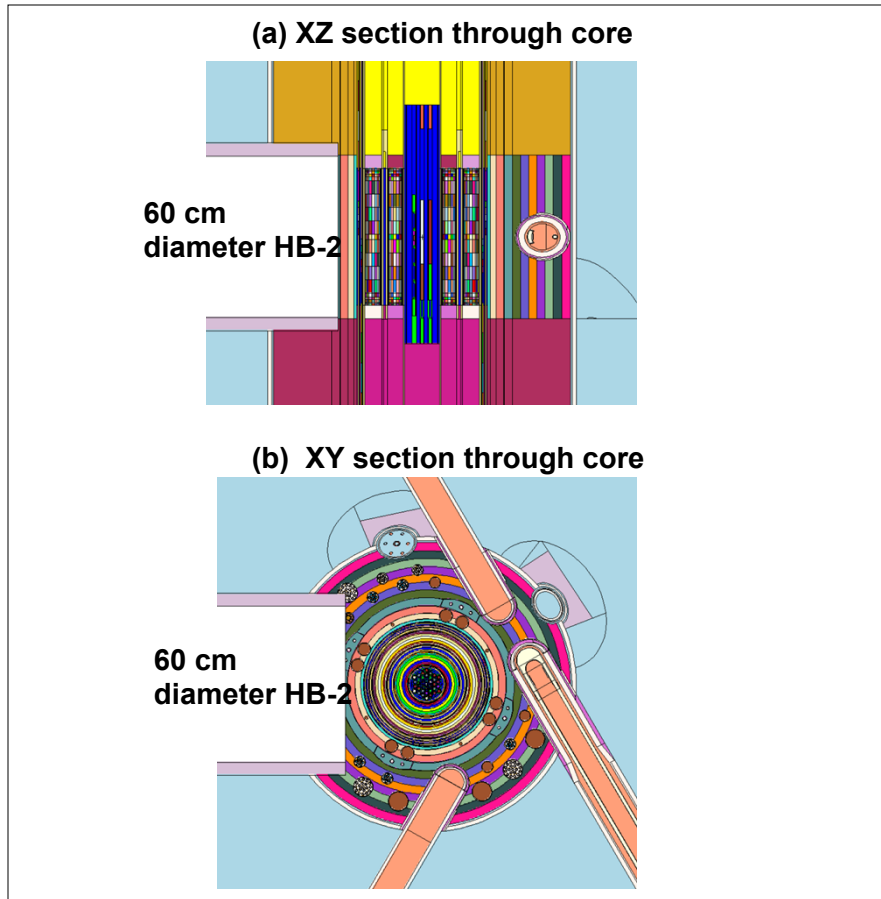


Figure 17. HFIR MCNP model with large HB-2 tube.

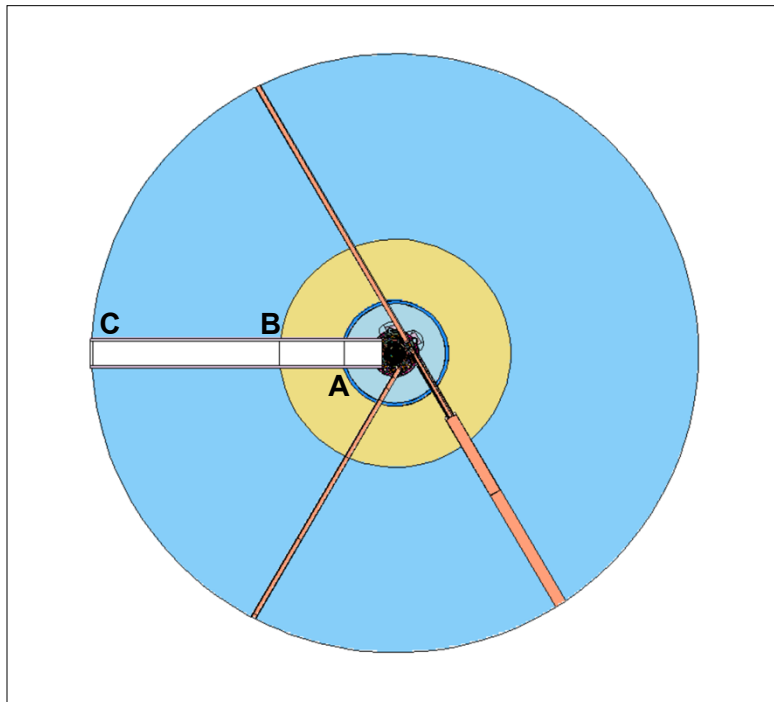


Figure 18. HFIR MCNP model with large HB-2 tube.

**Table 4. Neutron currents and fluxes for 60 cm diameter HB-2 concept.**

Location	Forward neutron current (n.s <sup>-1</sup> )			Estimated forward fluxes (n.cm <sup>-2</sup> .s <sup>-1</sup> ) (cross sectional area = 3,827 cm <sup>2</sup> )		
	Thermal	Fast	Total	Thermal	Fast	Total
A	1.52E+16	9.92E+16	1.14E+17	5.37E+12	3.51E+13	4.05E+13
B	3.77E+15	2.03E+16	2.40E+16	1.33E+12	7.17E+12	8.50E+12
C	1.24E+14	1.07E+15	1.20E+15	4.38E+10	3.80E+11	4.23E+11

Table 4 shows that the larger HB-2 tube meets the desired minimum impinging thermal neutron current specification of 1E14 n.s<sup>-1</sup> at beam tube exit point C. The neutron currents at points B and A are now in the region of 3E+15 and 1.5E16 n.s<sup>-1</sup>, with point A exceeding the upper neutron current requirement of 1E16 n.s<sup>-1</sup>. Therefore, using a larger tube shows promise, but major changes in the beryllium reflector, pressure vessel, and biological shield would be required.

One less invasive option would be to install a large thermal column with a UCN converter on HB-2 between the reactor vessel and the biological shield while keeping the HB-2 diameter and the biological shield penetration diameter unchanged. The large tube would utilize a 5E14 n.s<sup>-1</sup> current at location A and may be able to collect additional neutrons in a neutron flux of 1E12 n.cm<sup>-2</sup>.s<sup>-1</sup> (see minimum on Figure 14) outside the vessel. Another option would be to consider installing a large thermal column and converter between the vessel and the biological shield—*not* on one of the beam tubes. This option would have the least impact on the reactor itself, but it could pose other challenges with UCN collection and UCN beam line engineering.

### 3.4.6.3 Neutron Currents on EF-1

The EF-1 facility is one of HFIR's slanted experimental facilities situated behind HB-1 and HB-4, as shown in Figure 19. The tube partially penetrates the beryllium reflector and extends upward at an angle, penetrating the pressure vessel and biological shield, and then the tube opens up to a room in the reactor building, as illustrated in Figure 20.

The neutron currents were calculated for the existing 4 in. diameter tube and a conceptual larger 7 in. diameter tube. The results for these two cases shown in Figure 21 indicate that the larger diameter tube gives a higher neutron current of about 1E+12 n.s<sup>-1</sup> at the beam tube exit as opposed to the 2E+9 n.s<sup>-1</sup> for the 4 in. diameter tube. However, this current is still two orders of magnitude lower than the desired minimum of 1E+14 n.s<sup>-1</sup>. The existing EF-1 exit current is also two orders of magnitude lower than the neutron currents available on any existing HB beam tubes. To meet the neutron current requirement, the UCN converter would have to be installed inside the reactor vessel, where neutron currents of approximately 1.8E+14 would be accessible with a 7 in. diameter tube.

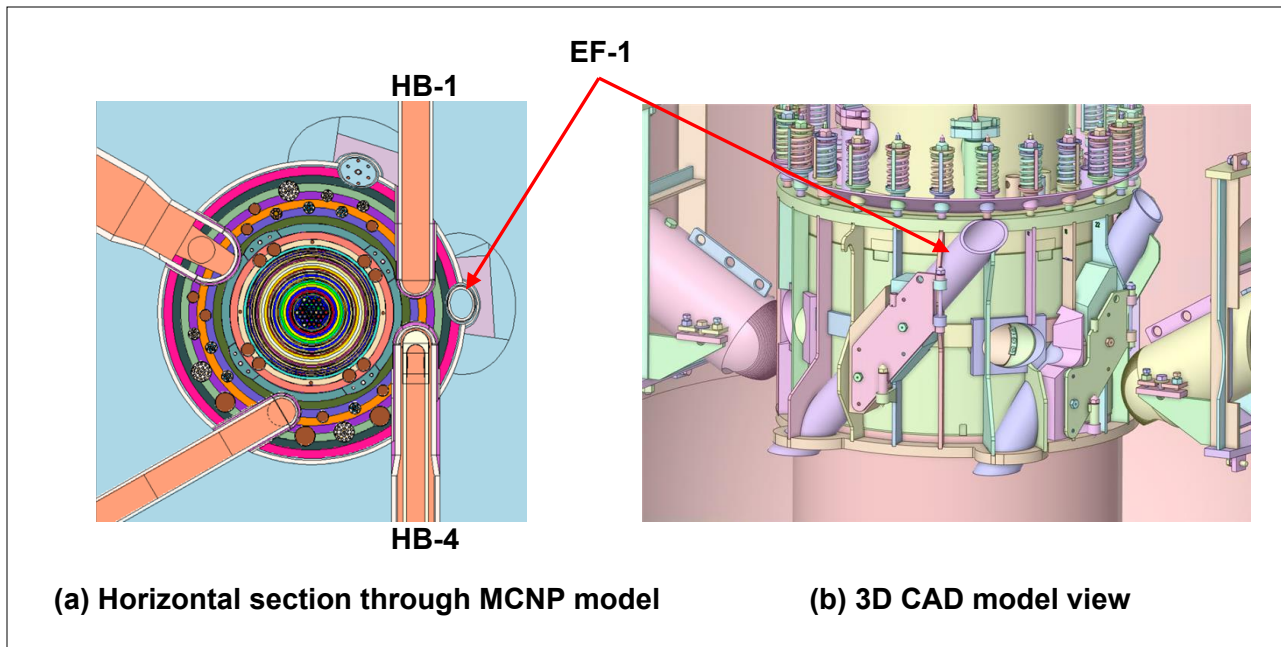


Figure 19. EF-1 facility.

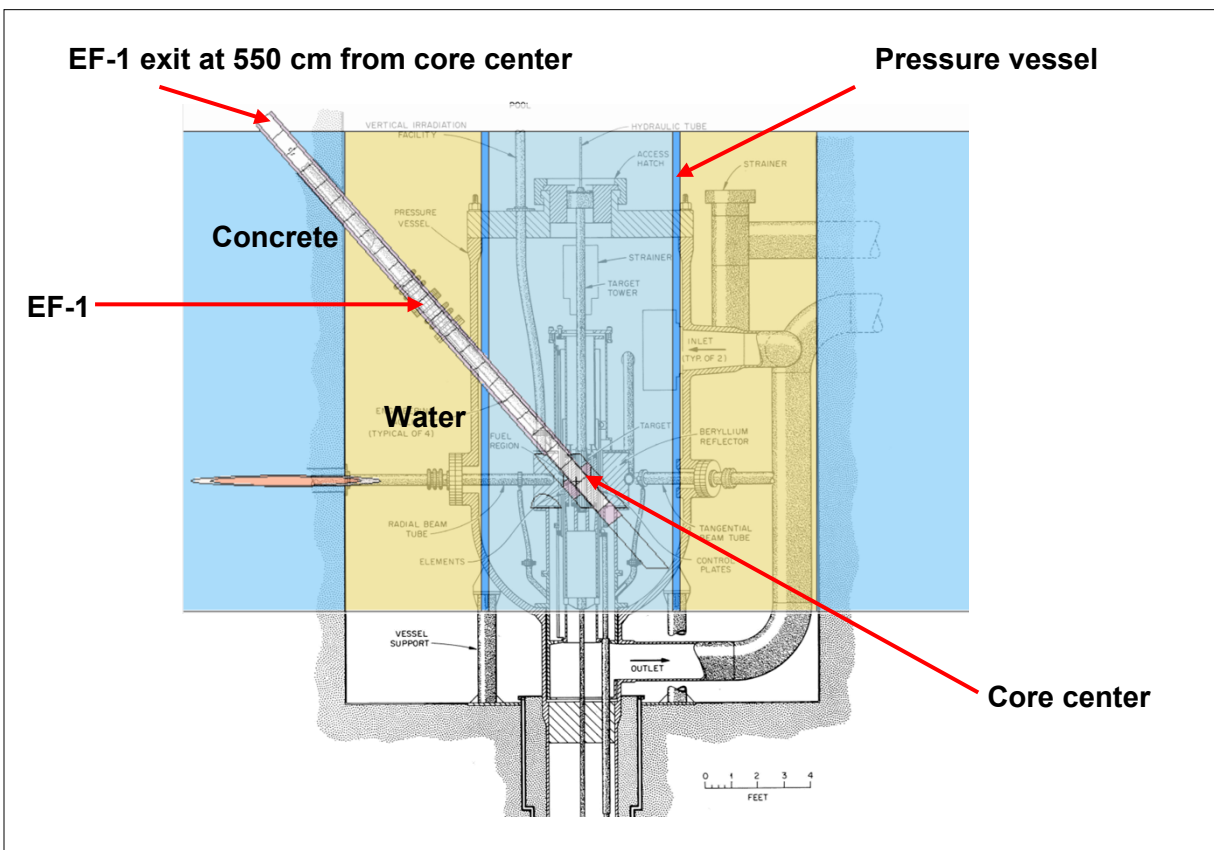


Figure 20. EF-1 Facility with MCNP model overlayed onto HFIR drawing.



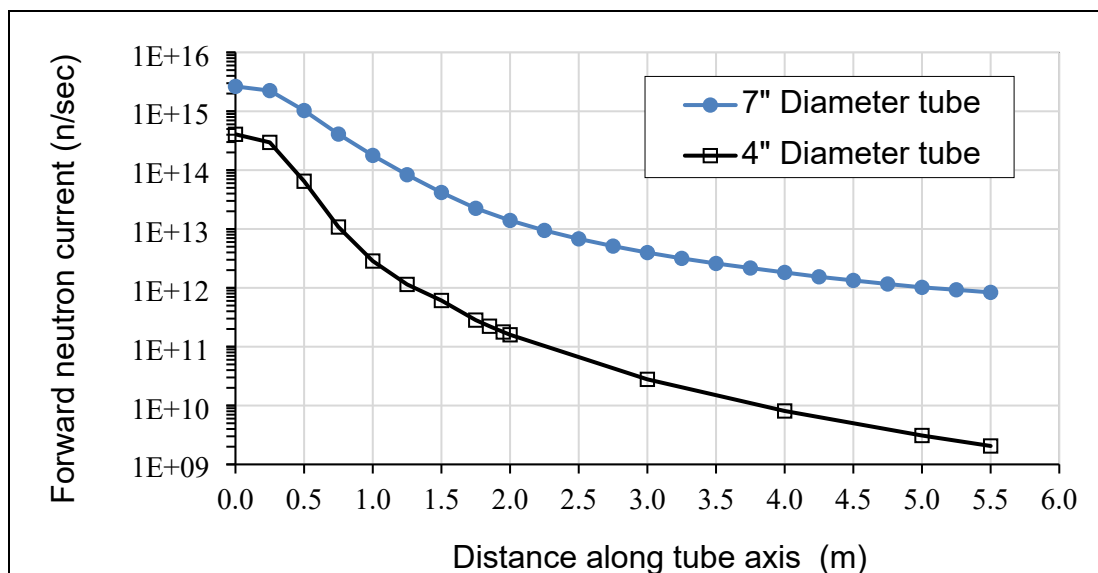


Figure 21. EF-1 neutron current results.

#### 3.4.6.4 Conclusion from scoping analyses

HFIR possesses the neutron flux levels required to generate UCNs of low densities (i.e., a few tens). However, HFIR does not have the capability to generate large UCN densities ( $13,000 \text{ UCN} \cdot \text{cm}^{-3}$ ) without modifications. In general, the required changes include larger beam tubes and a UCN converter positioned as close to the core as possible. Conceptual designs on HB-2 and EF-1, both with larger diameter tubes, could likely provide the necessary thermal source, and the UCN converter would be installed as close to the core as possible. Another possible option might be to install a large thermal column with the converter between the reactor vessel and the biological shield—*not* using one of the beam tubes. Based on these factors, there is potential to install an advanced UCN source at HFIR.

## 4. CONCLUSION

HFIR is a world leading facility with missions in isotope production, neutron scattering, and materials irradiation. This working group considered how additional detection systems could enhance and expand these missions. The team determined that rapid access detection systems, nonscattering beamline instruments, and an ultracold neutron source are the best candidates to add world-leading capabilities to HFIR. Through additional investment, HFIR's existing capabilities can be expanded to gain more scientific understanding and have the potential to provide best-in-class user facilities at ORNL.

## 5. REFERENCES

- Allmond, J.M. 2016. "Investigating Shape Evolution and the Emergence of Collectivity through the Synergy of Coulomb Excitation and  $\beta$  Decay." *EPJ Web of Conferences*: 123. EDP Sciences.
- Artnak, E.J., et al. 2018. "Development of Boron Calibration via Hybrid Comparator Method in Prompt Gamma Activation Analysis." *Journal of Radioanalytical & Nuclear Chemistry*. 318(1): 271–277.
- Belgya, T. 2012. "Prompt Gamma Activation Analysis at the Budapest Research Reactor." *Physics Procedia* 31: 99–109.

- Bergeron, A., B. Dionne, and T. Calzavara. 2014. *Neutronics Conversion Analyses of the Laue-Langevin Institute (ILL) High Flux Reactor (RHF)*, Argonne National Laboratory, ANL/GTRI/TM-14/15.
- BESAC 2020. Report of the Basic Energy Sciences Advisory Committee, “The Scientific Justification for a U.S. Domestic High-Performance Reactor-Based Research Facility,” US Department of Energy Office of Science. (<https://doi.org/10.2172/1647598>)
- Blanc, A., et al. 2013. “Fission Product Prompt  $\gamma$ -ray Spectrometer: Development of an Instrumented Gas-Filled Magnetic Spectrometer at the ILL.” *Nuclear Instruments and Methods in Physics Research Section B: Beam Interactions with Materials and Atoms* 317: 333–337.
- Borge, M.J.G. and K. Riisager. 2016. “HIE-ISOLDE, the Project and the Physics Opportunities.” *The European Physical Journal A* 52.11: 1–20.
- Bison, G., et al. 2016. Comparison of Ultracold Neutron Sources for Fundamental Physics Measurements, arXiv:1610.08399v1.
- Bryan, C.D. and D. Chandler 2022 (forthcoming). *The Future of Non-Scattering Science Capabilities at the High Flux Isotope Reactor (HFIR): Introduction to HFIR and the HFIR Sustaining and Enhancing Neutron Science (SENSe) Initiative*, Oak Ridge National Laboratory.
- Ceccio, G., et al. 2020. “Distribution of Lithium in Doped Nuclear Pores of Polyethylene Terephthalate by Neutron Depth Profiling.” *Radiation Effects and Defects in Solids* 175(3-4): 325–331.
- Ceccio, G., et al. 2020 “Measurement of Lithium Diffusion Coefficient in Thin Metallic Multilayer by Neutron Depth Profiling.” *Surface Interface Analysis* 52: 939–942.
- Chanjuan, T., et al. 2019. “Neutron Depth Profiling System at CARR”. *Applied Radiation and Isotopes* 148: 102–107.
- Cloet, I., and B. Kay. 2020. *Physics Division Strategic Plan Fiscal Years 2020–2024*. No. ANL-20/27. Argonne National Lab. (ANL), Argonne, IL.
- Downing, R.G. and G.P. Lamaze. 1995. “Near-Surface Profiling of Semiconductor Materials Using Neutron Depth Profiling.” *Semiconductor Science and Technology* 10(11): 1423–1431.
- Eberhardt, K. and C. Geppert. 2019. “The Research Reactor TRIGA Mainz – A Strong and Versatile Neutron Source for Science And Education,” *Radiochim. Acta* 107(7): 535–546.
- Fernández, M.V.V.. 2019. “Fast-Timing Investigation with  $\text{LaBr}_3$  (Ce) Arrays: Detector Optimization and Measurements in  $^{136}\text{Te}$ .” Universidad Complutense De Madrid.
- Frei, A. 2022. “The Source for Ultra-Cold Neutrons at the FRM II,” *Journal of Neutron Research*, In press.
- FRIB Decay Station Initiator (FDSi) Proposal, <https://fds.ornl.gov/documents/>
- FRIB Decay Station (FDS) White Paper, <https://fds.ornl.gov/documents/>
- FRM II Ultra-Cold Source. 2022. <https://www.frm2.tum.de/en/frm2/secondary-sources/ultra-cold-source/>, accessed 9/21/2022.
- Fukushima, M., H. Matsue, and A. Chatt. 2014. “A Feasibility Study to Measure Low Levels of Boron in Selected Canadian and Japanese Foods by Prompt Gamma Activation Analysis Using the JAEA JRR-3 Facility.” *Journal of Radioanalytical and Nuclear Chemistry* 302(3): 1225–1229.
- Goetz, K.C. *Total Absorption Spectroscopy of Neutron Rich Nuclei across the  $N=50$  Neutron Shell Closure*, Dissertation, University of Tennessee, 2017.
- Gray, T.J. et al. 2022. Nucl. Instrum. Methods Phys. Res., Sect. A, to be submitted (2022).

- Gross C.G. et al. 2000. "Performance of the recoil mass spectrometer and its detector systems at the holifield radioactive ion beam facility." *Nucl. Instrum. Methods Phys. Res., Sect. A* 450, 12-29.
- IAEA. *Development of an Integrated Approach to Routine Automation of Neutron Activation Analysis*, IAEA TECDOC-1839, International Atomic Energy Agency, Vienna, Austria, 2018.
- Institut Laue-Langevin - ILL, <https://www.ill.eu/users/instruments/instruments-list/pf2/technical-details>, accessed 9/21/2022.
- Johns, P.M., and J.C. Nino. 2019. "Room Temperature Semiconductor Detectors for National Security," *J. Appl. Phys.* 126, 040902.
- Jwa, Y.-J., et al. 2018. "Application of Prompt Gamma Activation Analysis to Provenance Study of the Korean Obsidian Artefacts." *Journal of Archaeological Science: Reports* 20: 374–381.
- Kirch, K. and P. Schmidt-Wellenburg. 2014. "Ultracold Neutron Sources and Neutron Electric Dipole Moment Experiments," *Conference Proceedings Fundamental Physics Using Atoms*, Tokyo, Japan.
- Kluge, E.J. et al. 2018. "Archaeometry at the PGAA Facility of MLZ – Prompt Gamma-Ray Neutron Activation Analysis and Neutron Tomography." *Journal of Archaeological Science: Reports* 20: 303–306.
- Korobkina, E., et al. 2007. "An Ultracold Neutron Source at the NC State University PULSTAR Reactor," *Nuclear Instruments and Methods in Physics Research A* 579: 530–533.
- Landsberger, S. 2005. "Handbook of Prompt Gamma Activation Analysis with Neutron Beams." *Journal of the American Chemical Society* 39: 13740.
- Lindstrom, R. and Z. Révay. 2017. "Prompt Gamma Neutron Activation Analysis (PGAA): Recent Developments and Applications." *Journal of Radioanalytical & Nuclear Chemistry* 314(2): 843–858.
- Linsenmann, F., et al. 2020. "A Liquid Electrolyte-Based Lithium-Ion Battery Cell Design for Operando Neutron Depth Profiling." *Journal of the Electrochemical Society* 167(10): 1–14.
- Livingston, R., et al. 2018. "Investigation of a Simulated Chinese Jade and Bronze Dagger-Axe by Neutron Radiography and Prompt Gamma Activation Analysis." *Journal of Archaeological Science: Reports* 21: 99–106.
- Mandal, R., et al. 2020. "Neutron Depth Profiling Using the Reactions  $^{10}\text{B}(n,\alpha)\text{Li-7}$  and  $^6\text{Li}(n,\alpha)\text{H-3}$  Induced by Thermal Neutrons." *Journal of Radioanalytical and Nuclear Chemistry*.
- Maróti, B., et al. 2020. "Joint Application of Structured-Light Optical Scanning, Neutron Tomography and Position-Sensitive Prompt Gamma Activation Analysis for the Non-Destructive Structural and Compositional Characterization Of Fossil Echinoids." *NDT and E International*. 115.
- Miura, T. and H. Matsue. 2016. "Precise Determination of Silicon in Ceramic Reference Materials by Prompt Gamma Activation Analysis at JRR-3." *Nuclear Engineering and Technology*. 48(2): 299–303.
- Mulligan, P.L., L.R. Cao, and D. Turkoglu. 2012. "A Multi-Detector, Digitizer Based Neutron Depth Profiling Device for Characterizing Thin Film Materials." *Review of Scientific Instruments*.
- Nagpure, S.C., et al. 2014. "Neutron Depth Profiling of Li-Ion Cell Electrodes with a Gas-Controlled Environment." *Journal of Power Sources* 248: 489–497.
- Otsuki, A., et al. 2109. "Non-Destructive Characterization of Mechanically Processed Waste Printed Circuit Boards: X-ray Fluorescence Spectroscopy and Prompt Gamma Activation Analysis." *Journal of Composites Science* 3(2): 54.

- Park, B.G., G.M. Sun, and H.D. Choi. 2014. “Development of Cold Neutron Depth Profiling System at HANARO.” *Nuclear Inst. and Methods in Physics Research, A* 752: 20–26.
- Paul, R.L., et al. 2015. “NGD Cold-Neutron Prompt Gamma-Ray Activation Analysis Spectrometer at NIST.” *Journal of Radioanalytical and Nuclear Chemistry* 304(1): 189–193.
- Petersburg Nuclear Physics Institute (PNPI), Jurchatov Institute,  
<http://www.pnpi.spb.ru/en/facilities/reactor-wwr-m>
- Petrov, Y.V., A. N. Erykalov, and M. S. Onegin. 2002. “The Fuel Cycle of Reactor PIK,” *International Meeting on Reduced Enrichment for Research and Test Reactors*, Bariloche, Argentina, November 3–8, 2002.
- Romano, C., R. Venkataraman, D. Glasgow, and B. Roach. 2022. “Measurement of the Effective Capture Cross Section of  $^{238}\text{Np}$  in the High Flux Isotope Reactor.” *Nucl. Technol.* DOI: 10.1080/00295450.2022.2070353.
- Savard, G. et al. 2015. “The CARIBU Facility.” *Proceedings of the Conference on Advances in Radioactive Isotope Science (ARIS2014)*
- Serebrov, A.P., et al. 2019. “Neutron Guide System for Ultracold and Cold Neutrons at the WWR-M Reactor,” *Technical Physics* 64(5) 737–744).
- Serebrov, A.P., et al. 2017. “UCN Source with Superfluid Helium at WWR-M Reactor,” *Journal of Physics: Conf. Series* 798, 012147.
- Serebrov, A.P., et al. 2016. “High-Density Ultracold Neutron Sources for the WWR-M and PIK Reactors,” *Crystallography Reports* 61 (1): 144–148.
- Serebrov, A.P., et al. 2016. “Program for Studying Fundamental Interactions at the PIK Reactor Facilities,” *Physics of Atomic Nuclei* 79(3): 293–303.
- Serebrov, A.P., et al. 2011. “Supersource of Ultracold Neutrons at WWR-M Reactor in PNPI and The Research Program on Fundamental Physics,” *Physics Procedia* 17, 251–258.
- Smodis, B., and L. Snoj. 2011. “Utilization and Application of the Slovenian TRIGA Reactor in ICORR: Safe Management and Effective Utilization.” IAEA-CN-188/A31, International Conference on Research Reactors: Safe Management and Effective Utilization, 14–18, Rabat, Morocco.
- Stieghorst, C. et al. 2018. “Determination of Boron and Hydrogen in Materials for Multicrystalline Solar Cell Production with Prompt Gamma Activation Analysis.” *Journal of Radioanalytical & Nuclear Chemistry* 317(1): 307–313.
- Szentmiklósi, L., et al. 2016. “Fifteen Years of Success: User Access Programs at the Budapest Prompt-Gamma Activation Analysis Laboratory.” *Journal of Radioanalytical & Nuclear Chemistry* 309(1): 71–77.
- Tomandl, I., et al. 2020. “Analysis of Li Distribution in Ultrathin All-Solid-State Li-Ion Battery (ASSLiB) by Neutron Depth Profiling (NDP).” *Radiation Effects and Defects in Solids* 175(3-4): 394–405.
- Trinks, U. F.J. Hartmann, S. Paul, and W. Schott. 2000. “Concepts of UCN Sources for the FRM-II,” *Nuclear Instruments and Methods in Physics Research A* 440: 666 – 673.
- Vezhlev, E., et al. 2020. “A New Neutron Depth Profiling Spectrometer at the JCNS for a Focused Neutron Beam.” *Radiation Effects and Defects in Solids* 175(3/4): 342–355.
- Wang, C., et al. 2017. “In Situ Neutron Depth Profiling of Lithium Metal–Garnet Interfaces for Solid State Batteries.” *Journal of the American Chemical Society* 139(40): 14257–14264.

- Werner, L., et al. 2018. “The New Neutron Depth Profiling Instrument N4DP at the Heinz Maier-Leibnitz Zentrum.” *Nuclear Inst. and Methods in Physics Research, A* 911: 30-36.
- Ziegler, J.F., G.W. Cole, and J.E.E. Baglin, “Technique for Determining Concentration Profiles of Boron Impurities in Substrates.” *J. Appl. Phys.* 1972. 43(9): 3809–3815.
- Zimmer, O., et al. 2011. 2011. “Superthermal Source of Ultracold Neutrons for Fundamental Physics Experiments,” *Phys. Rev. Lett.* 107, 134801.

